



# THE UNIVERSITY *of* EDINBURGH

## Edinburgh Research Explorer

### Rapamycin Regulates Autophagy and Cell Adhesion in Induced Pluripotent Stem Cells

**Citation for published version:**

Kunath, T, Sothibundhul, A, McDonagh, K, Von Kriegsheim, A, Garcia-Munoz, A, Klawiter, A, Thompson, K, Dev Chauhan, K, Krawczyk, J, McInerney, V, Dockery, P, Devine, MJ, Barry, F, O'Brien, T & Shen, S 2016, 'Rapamycin Regulates Autophagy and Cell Adhesion in Induced Pluripotent Stem Cells' *Stem Cell Research and Therapy*, vol. 7, no. 166. DOI: 10.1186/s13287-016-0425-x

**Digital Object Identifier (DOI):**

[10.1186/s13287-016-0425-x](https://doi.org/10.1186/s13287-016-0425-x)

**Link:**

[Link to publication record in Edinburgh Research Explorer](#)

**Document Version:**

Peer reviewed version

**Published In:**

Stem Cell Research and Therapy

**General rights**

Copyright for the publications made accessible via the Edinburgh Research Explorer is retained by the author(s) and / or other copyright owners and it is a condition of accessing these publications that users recognise and abide by the legal requirements associated with these rights.

**Take down policy**

The University of Edinburgh has made every reasonable effort to ensure that Edinburgh Research Explorer content complies with UK legislation. If you believe that the public display of this file breaches copyright please contact [openaccess@ed.ac.uk](mailto:openaccess@ed.ac.uk) providing details, and we will remove access to the work immediately and investigate your claim.



# Stem Cell Research & Therapy

## Rapamycin Regulates Autophagy and Cell Adhesion in Induced Pluripotent Stem Cells

--Manuscript Draft--

<b>Manuscript Number:</b>	SCRT-D-16-00129R1	
<b>Full Title:</b>	Rapamycin Regulates Autophagy and Cell Adhesion in Induced Pluripotent Stem Cells	
<b>Article Type:</b>	Research	
<b>Funding Information:</b>	Science Foundation Ireland (09/SRC B1794)	Prof Sanbing Shen
	Science Foundation Ireland (09/SRC/B1794s1)	Prof Sanbing Shen
	SFI Investigator Programme (13/IA/1787)	Prof Sanbing Shen
	SFI TIDA program (14/TIDA/2258)	Prof Sanbing Shen
	NUI Galway (RSU002)	Prof Sanbing Shen
<b>Abstract:</b>	<p>Background: Cellular reprogramming is a stressful process, which requires cells to engulf somatic features, produce and maintain stemness machineries. Autophagy is a process to degrade unwanted proteins and required for the derivation of induced pluripotent stem cells (iPSCs). However, the role of autophagy during iPSC maintenance remains undefined.</p> <p>Methods: Human iPSCs were investigated by microscopy, immunofluorescence and immunoblotting to detect autophagy machinery. Cells were treated with Rapamycin to activate autophagy and Bafilomycin to block autophagy during iPSC maintenance. High concentrations of Rapamycin treatment, unexpectedly, resulted in spontaneous formation of round floating spheres of uniform size, which were analyzed for differentiation into three germ layers. Mass spectrometry was deployed to reveal altered protein expression and pathways associated with Rapamycin treatment.</p> <p>Results: We demonstrate that human iPSCs express high basal levels of autophagy, including key components of APMK<math>\alpha</math>, ULK1/2, BECLIN-1, ATG13, ATG101, ATG12, ATG3, ATG5 and LC3B. Block of autophagy by Bafilomycin induces iPSC death and Rapamycin attenuates the Bafilomycin effect. Rapamycin treatment up-regulates autophagy in iPSCs in a dose/time-dependent manner. High concentration of Rapamycin reduces NANOG expression and induces spontaneous formation of round and uniformly sized embryoid bodies (EBs) with accelerated differentiation into three germ layers. Mass spectrometry analysis identifies actin cytoskeleton and adherens junctions as the major targets of Rapamycin in mediating iPSC detachment and differentiation.</p> <p>Conclusions: High levels of basal autophagy activity are present during iPSC derivation and maintenance. Rapamycin alters expression of actin cytoskeleton and adherens junctions, induces uniform EB formation and accelerates differentiation. iPSCs are sensitive to enzyme dissociation and require lengthy differentiation time. The shape and size of EBs also play a role in the heterogeneity of end cell products. Therefore, this research highlights the potential of Rapamycin in producing uniform EBs and in shortening iPSC differentiation duration.</p>	
<b>Corresponding Author:</b>	Sanbing Shen, BSc, MSc, PhD NUI Galway Galway, IRELAND	
<b>Corresponding Author Secondary Information:</b>		
<b>Corresponding Author's Institution:</b>	NUI Galway	
<b>Corresponding Author's Secondary Institution:</b>		
<b>First Author:</b>	Areechun Sothibundhu	
<b>First Author Secondary Information:</b>		

<b>Order of Authors:</b>	Areechun Sotthibundhu
	Katya McDonagh
	Alexander von Kriegsheim
	Amaya Garcia-Munoz
	Agnieszka Klawiter
	Kerry Thompson
	Kapil Dev Chauhan
	Janusz Krawczyk
	Veronica McInerney
	Peter Dockery
	Michael J Devine
	Tilo Kunath
	Frank Barry
	Timothy O'Brien
Sanbing Shen, BSc, MSc, PhD	
<b>Order of Authors Secondary Information:</b>	
<b>Response to Reviewers:</b>	<p>Point-to-point Response</p> <p>Reviewer reports:</p> <p>Reviewer #1: This is an interesting investigation into the role of autophagy in iPSC function, and builds on the growing body of work demonstrating the key role of autophagy in stem cell biology. The authors show a higher level of autophagy at basal conditions in iPSCs over their parental fibroblasts, which can be modulated in a dose-dependent manner with rapamycin to affect the iPSC maintenance in culture and EB formation/differentiation over time.  RESPONSE: We thank Reviewer #1 for careful reading and recognition of the key points of the manuscript.</p> <p>General comments:</p> <ul style="list-style-type: none"> <li>- The English in the manuscript would benefit from revision. Several areas are in need of editing for clarity, and there are a high number of errors/typos throughout the manuscript.  RESPONSE: We apology for the errors/typos in the previous versions. The Manuscript has now been gone through several edits and hope the revised version is substantially improved.</li> <li>- Avoid including discussion of the results in the Results section (e.g. discussion of the results in Fig 2)  RESPONSE: The introductory contents in section 2 and 3 of the Results on pages 11-12 are now shortened.</li> </ul> <p>Specific comments:</p> <p>I appreciated the demonstration of high LC3II levels across four separate donors in the iPSC population. I would perhaps suggest including LC3I levels at least in the blot in 2E to show whether there is an upregulation of autophagosome accumulation/cycling, or a block in autophagosome degradation that causes the shift. Some recent studies have shown stem cell populations to have very low degrees of autophagosome cycling at a basal state.  RESPONSE: We acknowledge that The Reviewer #1 brought up an interesting point of the autophagosome cycling. This manuscript has addressed several points: high level of the autophagy is crucial for iPSC physiology and maintenance, and induced autophagy by Rapamycin is associated with cell detachment and EB formation</p>

together with accelerated differentiation.

In the revised version, we have new data to further strengthen the importance of autophagy in iPSCs, that block of autophagy by Bafilomycin induces cell death and Rapamycin rescues Bafilomycin-induced cell death (See Lines 303-320 and new Figure 5). We also provide new mechanistic data for accelerated differentiation that Rapamycin downregulates NANOG expression in a concentration-dependent manner (See Figure 8L-M, and lines 355-362, 767-771).

We kept the original Figure 2 which was done on 10% SDS-PAGE. The data showed that (1) Rapamycin can induce autophagy in both iPSCs and fibroblasts, and (2) both the basal and induced autophagy activities are higher in iPSCs. We have now provided a Supplemental Figure 1 to show that two bands of LC3B-I (16kD) and LC3B-II (14kD) can be better resolved on 15% SDS-PAGE. The new data brought up an interesting point that Rapamycin increased LC3B-I rather than LC3B-II expression in fibroblasts (Supplemental Figure 1), and this is different from iPSCs (see Figure 4), and will require further investigation and is therefore provided as a Supplemental Figure, to avoid diversion of the focus. See Line 299-301.

: The overall goal of this figure seems to be to show high levels of autophagy signaling molecules across several iPSC lines. Demonstrating the activation of autophagy signaling is important, but it is difficult to discern levels of activation with no outside standard for comparison in this figure (all relative abundance measurements are made using each individual sample as its own control). I would suggest including a lane or two of parental fibroblasts or other control cells to serve as a comparison as you did in Figure 2.

RESPONSE: We appreciate Reviewer #1's comments, carried out new experiments and included new data in the revised Figure 3H. Consistent with other data shown in the manuscript, both ATG5 and ATG12 are more abundant in iPSCs than that in parental fibroblasts. See revised Figure 3H and lines 280-283

It is also unclear why samples a-e are assayed for ATGs but not f-i. Error bars are missing from Fig 3G.

RESPONSE: This reflected the history of iPSC availability in the group. We first carried out series of WB on 5 lines (a-e, see Figure 3A-B) with three repeated blots. When additional 7 iPSC lines "f-i" became available, we further strengthen the point by using iPSC line "b" as a reference in the new Western blots. These lines were done only once (Figure 3C and G), but the data were consistent with 5 lines in A-B, Figure 3A,B,D-F.

Fig 5/6: Results investigating the iPSC maintenance focus solely on the rapamycin dosing. Inhibition of autophagy with bafilomycin or another treatment is not discussed in this study much. If rapamycin benefits iPSC maintenance and differentiation, how does inhibiting the pathway affect things? Some studies on stem cell autophagy have shown conflicting roles of rapamycin and bafilomycin treatments on the function of autophagy.

RESPONSE: We appreciate Reviewer #1 for expert opinion. We carried out additional experiments with bafilomycin A1 as suggested. The new data showed that bafilomycin induced dose-dependent cell death whereas Rapamycin can rescue Bafilomycin-induced cell death (See lines 303-320 and new Figure 5). This further highlights the importance of autophagy in iPSCs.

Fig 8: Given that the authors showed an optimal Rapamycin response of 200 nM in Fig 4 and used this dose for subsequent EB experiments in Figs 5-7, it is unclear why 50 and 100 uM doses are used in this experiment, which are substantially higher doses.

RESPONSE: Apology for the typos. we used 50 and 100 nM (not uM) in proteomics assays.

Discussion: The discussion focuses largely on results from Fig 8, which seems minor compared to the rest of the manuscript that focuses on the specific autophagic character and response in the iPSCs examined here. Some points for consideration in the discussion:

- Fig 2 shows two donors having different basal levels of autophagy (a/b vs c/d). How will donor variability affect these results, or even different iPSC parent sources?

- Do the authors feel that a particular set of culture conditions here are suitable for recommended use in standard iPSC culture? How should rapamycin be used most efficiently to benefit iPSC maintenance, differentiation, etc?

- EBs assayed in Fig 7 show a high level of LC3-I compared to the control EBs. Speculation as to why? How does the basal level of cytosolic LC3/autophagosome cycling and accumulation affect this function of iPSCs?

RESPONSE: many thanks to Reviewer 1 for constructive advice. We revised Discussion accordingly

Reviewer #2: The manuscript by Sothibundhu A and colleagues describes that inhibition of mTOR signaling pathway by rapamycin could regulates autophagy and cell adhesion in induced pluripotent stem cells. The group highlights that the potential of rapamycin in producing uniform embryoid bodies and in accelerating iPSCs differentiation.

Overall, the manuscript is interesting and will contribute to the current understanding of iPSCs biology. It is of particular interest and may encourage further studies into this area about the role of autophagy during iPSC maintenance. However, the work as developed is largely confirmatory of previous findings and while there is some new information, such is limited. For example, it is well established that autophagy could be regulated by mTOR pathway, and regulation of embryoid body formation by mTOR pathway was also reported (Oncogene 2010).

RESPONSE: We thank Reviewer #2 for bringing up this literature, which is different from our data with different cell types. The paper is cited as Ref 40 and discussed in lines 413-416 .

My critiques:

1. In figure 1A, images showing autophagic vacuoles of fibroblasts without reprogramming should also be shown. In panel H-K, its better to show the colocalization of autophagy, lysosome, Golgi and ER markers in the same cell

RESPONSE: Thank Reviewer #2 for constructive comments. We now added a bright field image of fibroblasts in new Figure 1F. We carried out double staining as suggested and included in new Figure 1C,D,G,H.

2. In figure 2F&G, it seems that LC3BII in iPSCs showed similar increase (about 2.5 folds) that fibroblasts, no matter the cells were treated with rapamycin or not. How it can be concluded that autophagy is rapamycin-inducible?

RESPONSE: Figure 2F showed the difference of basal LC3B between fibroblasts and iPSCs. Figure 2G showed relative LC3B activity between fibroblasts and iPSCs after Rapamycin treatment. Rapamycin can induce LC3B in both fibroblasts and iPSCs. See lines 255-265.

3. In figure 3, the results of fibroblasts as negative control should also be shown.

RESPONSE: Thank Reviewer #2 for the suggestion. I have now included new data on Figure 3H, showing ATG5 and ATG12 are higher in iPSCs than in fibroblasts.

4. The figure 5F and figure 6E are the same image, please change either of them

RESPONSE: Many thanks to Reviewer #2 for careful reading. We have now removed the duplicated image, see revised Figure 7.

5. What's the difference among figure 7J, K and L?

RESPONSE: Many thanks. We have now removed K and L, and added new mechanistic data of reduced NANOG expression by Rapamycin treatment see revised Figure 8.

[Click here to view linked References](#)

# 1 **Rapamycin Regulates Autophagy and Cell Adhesion in Induced Pluripotent Stem Cells**

2  
3 2 Areechun Sotthibundhu<sup>1,8</sup>, Katya McDonagh<sup>1</sup>, Alexander von Kriegsheim<sup>2</sup>, Amaya Garcia-  
4  
5 3 Munoz<sup>2</sup>, Agnieszka Klawiter<sup>1</sup>, Kerry Thompson<sup>3</sup>, Kapil Dev Chauhan<sup>1</sup>, Janusz Krawczyk<sup>4</sup>  
6  
7  
8 4 Veronica McInerney<sup>5</sup>, Peter Dockery<sup>3</sup>, Michael J Devine<sup>6,7</sup>, Tilo Kunath<sup>6</sup>, Frank Barry<sup>1</sup>,  
9  
10 5 Timothy O'Brien<sup>1</sup>, Sanbing Shen<sup>1\*</sup>

11  
12  
13 6 <sup>1</sup> Regenerative Medicine Institute, School of Medicine, National University of Ireland (NUI)  
14  
15 Galway, Galway, Ireland.

16  
17  
18 8 <sup>2</sup> Systems Biology Ireland, Conway Institute, University College Dublin, Dublin 4, Ireland

19  
20  
21 9 <sup>3</sup> Centre for Microscopy and Imaging, Anatomy, School of Medicine, NUI Galway, Ireland

22  
23  
24 10 <sup>4</sup> Department of Haematology, Galway University Hospital

25  
26 11 <sup>5</sup> HRB Clinical Research Facility, NUI Galway, University Road, Galway Ireland

27  
28  
29 12 <sup>6</sup> MRC center for Regenerative Medicine, The University of Edinburgh, UK

30  
31 13 <sup>7</sup> Department of Molecular Neuroscience, Institute of Neurology, University College London,  
32  
33 London WC1N 3BG, UK

34  
35  
36 15 <sup>8</sup> Chulabhorn International College of Medicine, Thammasat University, Patumthani, 12120,  
37  
38 Thailand

39  
40  
41 17 Email addresses: [areechuns@gmail.com](mailto:areechuns@gmail.com); [katya.mcdonagh@gmail.com](mailto:katya.mcdonagh@gmail.com);

42  
43 18 [kriegsheim@gmail.com](mailto:kriegsheim@gmail.com); [Amaya.GarciaMunoz@ucd.ie](mailto:Amaya.GarciaMunoz@ucd.ie); [a.klawiter.08@aberdeen.ac.uk](mailto:a.klawiter.08@aberdeen.ac.uk);

44  
45 19 [Kerry.Thompson@nuigalway.ie](mailto:Kerry.Thompson@nuigalway.ie); [kapil.dev@nuigalway.ie](mailto:kapil.dev@nuigalway.ie); [Janusz.Krawczyk@hse.ie](mailto:Janusz.Krawczyk@hse.ie);

46  
47 20 [Veronica.Mcinerney@nuigalway.ie](mailto:Veronica.Mcinerney@nuigalway.ie); [Peter.Dockery@nuigalway.ie](mailto:Peter.Dockery@nuigalway.ie);

48  
49 21 [michael.devine.09@ucl.ac.uk](mailto:michael.devine.09@ucl.ac.uk); [tilo.kunath@ed.ac.uk](mailto:tilo.kunath@ed.ac.uk); [frank.barry@nuigalway.ie](mailto:frank.barry@nuigalway.ie);

50  
51 22 [timothy.obrien@nuigalway.ie](mailto:timothy.obrien@nuigalway.ie); [sanbing.shen@nuigalway.ie](mailto:sanbing.shen@nuigalway.ie).

52  
53 23 \* Corresponding author: Sanbing Shen, Regenerative Medicine Institute, School of Medicine,  
54  
55 NUI Galway, Galway, Ireland, Tel:+353 91 494261, email: [sanbing.shen@nuigalway.ie](mailto:sanbing.shen@nuigalway.ie)

25 **Abstract**

1  
2  
3 26 **Background:** Cellular reprogramming is a stressful process, which requires cells to engulf  
4  
5 27 somatic features, produce and maintain stemness machineries. Autophagy is a process to  
6  
7 28 degrade unwanted proteins and required for the derivation of induced pluripotent stem cells  
8  
9 29 (iPSCs). However, the role of autophagy during iPSC maintenance remains undefined.

10  
11  
12 30 **Methods:** Human iPSCs were investigated by microscopy, immunofluorescence and  
13  
14 31 immunoblotting to detect autophagy machinery. Cells were treated with Rapamycin to activate  
15  
16 32 autophagy and Bafilomycin to block autophagy during iPSC maintenance. High concentrations  
17  
18 33 of Rapamycin treatment, unexpectedly, resulted in spontaneous formation of round floating  
19  
20 34 spheres of uniform size, which were analyzed for differentiation into three germ layers. Mass  
21  
22 35 spectrometry was deployed to reveal altered protein expression and pathways associated with  
23  
24 36 Rapamycin treatment.

25  
26  
27 37 **Results:** We demonstrate that human iPSCs express high basal levels of autophagy, including  
28  
29 38 key components of APMK $\alpha$ , ULK1/2, BECLIN-1, ATG13, ATG101, ATG12, ATG3, ATG5  
30  
31 39 and LC3B. Block of autophagy by Bafilomycin induces iPSC death and Rapamycin attenuates  
32  
33 40 the Bafilomycin effect. Rapamycin treatment up-regulates autophagy in iPSCs in a dose/time-  
34  
35 41 dependent manner. High concentration of Rapamycin reduces NANOG expression and induces  
36  
37 42 spontaneous formation of round and uniformly sized embryoid bodies (EBs) with accelerated  
38  
39 43 differentiation into three germ layers. Mass spectrometry analysis identifies actin cytoskeleton  
40  
41 44 and adherens junctions as the major targets of Rapamycin in mediating iPSC detachment and  
42  
43 45 differentiation.

44  
45  
46 46 **Conclusions:** High levels of basal autophagy activity are present during iPSC derivation and  
47  
48 47 maintenance. Rapamycin alters expression of actin cytoskeleton and adherens junctions,  
49  
50 48 induces uniform EB formation and accelerates differentiation. iPSCs are sensitive to enzyme



1  
2  
3  
4  
5 49 dissociation and require lengthy differentiation time. The shape and size of EBs also play a role  
6  
7  
8 50 in the heterogeneity of end cell products. Therefore, this research highlights the potential of  
9  
10  
11 51 Rapamycin in producing uniform EBs and in shortening iPSC differentiation duration.  
12  
13

14  
15  
16  
17  
18  
19  
20  
21  
22 52  
23  
24  
25  
26  
27  
28  
29  
30  
31  
32  
33  
34  
35  
36  
37  
38  
39  
40  
41  
42  
43  
44  
45  
46  
47  
48  
49  
50  
51  
52  
53  
54  
55  
56  
57  
58  
59  
60  
61  
62  
63  
64  
65  
66  
67  
68  
69  
70  
71  
72  
73  
74  
75  
76  
77  
78  
79  
80  
81  
82  
83  
84  
85  
86  
87  
88  
89  
90  
91  
92  
93  
94  
95  
96  
97  
98  
99  
100  
101  
102  
103  
104  
105  
106  
107  
108  
109  
110  
111  
112  
113  
114  
115  
116  
117  
118  
119  
120  
121  
122  
123  
124  
125  
126  
127  
128  
129  
130  
131  
132  
133  
134  
135  
136  
137  
138  
139  
140  
141  
142  
143  
144  
145  
146  
147  
148  
149  
150  
151  
152  
153  
154  
155  
156  
157  
158  
159  
160  
161  
162  
163  
164  
165

53 **Key words**

54 Actin cytoskeleton, Adherens junctions, Autophagy, Differentiation, Embryoid Body, Induced  
55 Pluripotent Stem Cells, Rapamycin

56  
57  
58  
59  
60  
61  
62  
63  
64  
65  
66  
67  
68  
69  
70  
71  
72  
73  
74  
75  
76  
77  
78  
79  
80  
81  
82  
83  
84  
85  
86  
87  
88  
89  
90  
91  
92  
93  
94  
95  
96  
97  
98  
99  
100  
101  
102  
103  
104  
105  
106  
107  
108  
109  
110  
111  
112  
113  
114  
115  
116  
117  
118  
119  
120  
121  
122  
123  
124  
125  
126  
127  
128  
129  
130  
131  
132  
133  
134  
135  
136  
137  
138  
139  
140  
141  
142  
143  
144  
145  
146  
147  
148  
149  
150  
151  
152  
153  
154  
155  
156  
157  
158  
159  
160  
161  
162  
163  
164  
165

57 **Background**

58 The induced pluripotent stem cell (iPSC) technology enables conversion of patient's somatic  
59 cells into embryonic stem (ES)-like cells [1], which can be differentiated into the major cell  
60 types in the body, raising the expectation of personalized medicine to treat patients with own  
61 somatic tissue-derived cells. This also offers an opportunity to generate human cell models of  
62 diseases for therapeutic development, which has not kept pace with pharmaceutical investment in  
63 recent decades. A major impediment to drug discovery is attributable to the lack of suitable  
64 disease models of human origin, as species differences may totally affect drug efficacy [2]. Some  
65 disease pathologies are shown to be re-capitulated in the culture dish. For example, many  
66 patient-specific iPSCs have been generated to investigate disease progression *in vitro* and  
67 disease-related phenotypes are partially preserved in iPSC-derived cells [3-6]. Recent successes  
68 in the growth of "mini-organ", i.e., 3D retina [7-8] and cerebral organoids [9], may provide 3-D  
69 human disease models. However, there are challenges in phenotyping iPSCs prior to the  
70 development of screening assays, which include lengthy differentiation durations and  
71 heterogeneity of the end cell products.



1  
2  
3  
4  
5  
6  
7  
8  
9  
10  
11  
12  
13  
14  
15  
16  
17  
18  
19  
20  
21  
22  
23  
24  
25  
26  
27  
28  
29  
30  
31  
32  
33  
34  
35  
36  
37  
38  
39  
40  
41  
42  
43  
44  
45  
46  
47  
48  
49  
50  
51  
52  
53  
54  
55  
56  
57  
58  
59  
60  
61  
62  
63  
64  
65

72 The differentiation, survival and self-renewal of human stem cells can be regulated by a 3D  
73 microenvironment including shape and size [7-9,10]. Human iPSCs are hyper-sensitive to cell  
74 dissociation reagents, and seconds of exposure to Trypsin/EDTA may lead to failure of iPSC  
75 adhesion or survival. Consequently, many laboratories adopt “cut-and-paste” method to  
76 mechanically passage iPSCs, which results in EBs of uncontrollable sizes with irregular shapes,  
77 which may potentially contribute to the heterogeneity. The differentiation of mature cell types  
78 from human iPSCs is also time-consuming. For example, 3~5 months are required to generate  
79 functional neurons, astrocytes or oligodendrocytes [11-13]. Therefore, accelerated differentiation  
80 remains to be optimized.

81 Efforts have been made to improve the reprogramming efficiency, and autophagy, a process to  
82 degrade unwanted proteins, is found as one of the regulators during cellular reprogramming [14-  
83 15]. Autophagy is conserved from yeast to mammals, and is generally induced by intra- and  
84 extra-cellular stress. Upon induction, the preautophagosomal structure is formed and elongated  
85 to form a phagophore, which engulfs cytoplasmic components, leading to the formation of  
86 autophagosomes with double membranes. The genes involved in the autophagy are termed  
87 Autophagy-Related Genes (*ATGs*), and >12 *ATGs* have been identified. They regulate  
88 autophagosome formation through two evolutionarily conserved ubiquitin-like conjugation  
89 systems, the ATG12-ATG5 and the ATG8 (LC3)-PE (phosphatidylethanolamine) systems [16].  
90 The LC3B-I (microtubule-associated proteins 1A/1B light chain 3-I) is conjugated with PE to  
91 become LC3B-II, which associates with both the outer and inner membranes of the  
92 autophagosome. After fusion with the lysosome, the autolysosome is degraded [17]. In mice,  
93 Atg3, Atg5 and Atg7 are essential for reprogramming of mouse embryonic fibroblasts [14-15].  
94 Cells lacking Atg3, Atg5 or Atg7 abrogated iPSC colony formation [15].

95 The autophagy pathway can be activated by AMPK signaling, but is normally inhibited by the  
96 mammalian target of the Rapamycin (mTOR) pathway. The presence of hyperactivated mTOR

1 97 activity in *Tsc2*<sup>-/-</sup> somatic cells completely blocked reprogramming [14]. Consistent with this,  
2  
3 98 Rapamycin - an inhibitor of the mTOR pathway at 0.3-1 nM could increase reprogramming  
4  
5 99 efficiency by 2~3 folds [18]. In addition, 0.1 nM of PP242, a selective inhibitor of  
6  
7 100 mTORC1/mTORC2 binding at the ATP domain, also increased reprogramming efficiency by 5-  
8  
9 101 folds [18]. Other compounds associated with autophagy such as PQ401- an IGF1 receptor  
10  
11 102 inhibitor and LY294002 - an inhibitor of PI3K also increased reprogramming by 4-folds [18].  
12  
13  
14 103 Mechanistically, mTOR is regulated by SOX2, one of the four reprogramming factors. SOX2  
15  
16 104 can physically bind to the mTOR promoter and repress mTOR expression thereby activate  
17  
18  
19 105 autophagy [15]. Therefore, an appropriate level of autophagy is required for cell reprogramming.  
20  
21  
22 106 However, roles of autophagy in iPSC maintenance and differentiation remain elusive.

23  
24  
25 107 In this study, we showed the presence of high levels of basal autophagy activity during iPSC  
26  
27 108 reprogramming and maintenance. Rapamycin alters expression of adherens junctions and actin  
28  
29  
30 109 cytoskeleton, induces iPSC detachment, and results in uniform EB formation. Rapamycin  
31  
32 110 treatment also accelerates differentiation of human iPSCs into three germ-layers.  
33  
34  
35

36 111

## 37 38 39 112 **Methods**

### 40 41 42 43 113 **iPSC derivation**

44  
45  
46 114 On day 0, human fibroblasts were seeded at a density of  $2.0 \times 10^4$  cells/well on a 6-well dish. Next  
47  
48  
49 115 day, cells were transduced with a polycistronic (OKSM) lentivirus containing four  
50  
51 116 reprogramming factors (SCR544- Human STEMCCA constitutive lentivirus reprogramming kit,  
52  
53  
54 117 Millipore, SCR544) in 700  $\mu$ l of fibroblast medium, supplemented with 4 $\mu$ g/ ml polybrene  
55  
56 118 (Millipore, TR-1003). On day 2, cells were repeatedly transduced with lentivirus. The medium  
57  
58  
59 119 was then replaced daily with complete fibroblast medium supplemented with 0.25 mM sodium

120 butyrate (NaB, Sigma, 156-54-7) for 4 days. On day 6, 6-well dishes were pre-seeded with  $\gamma$ -  
121 irradiated MEF (VH Bio Limited, 07GSC6001G) at a density of  $1.5 \times 10^5$  cells/well. On day 7,  
122 transduced cells were trypsinized with 0.25% Trypsin/EDTA, and replated onto pre-seeded MEF  
123 dishes at a density of  $3.0 \times 10^4$  cells/well, and cultured in KO iPSC medium supplemented with  
124 10ng/ml bFGF (Peprotech, 100-18B) plus 0.25 mM NaB. The medium was changed every other  
125 day. The addition of NaB was discontinued after day 20.

126 Individual iPSC colonies began to emerge after day 14 and were picked up on day 28,  
127 mechanically dissociated into smaller pieces by pipetting and plated into  $\gamma$ -MEF coated 12-well  
128 plates. Selected clones were characterized using alkaline phosphatase activity, RT-PCR and  
129 immunoblotting to detect endogenous expression of OCT4, SOX2 and NANOG, and  
130 immunocytochemistry to detect surface markers of SSEA4, TRA 1-60 and TRA 1-81 in addition  
131 to the transcription factors (StemLight™ pluripotency antibody kit, cell signaling, 9656).

## 132 Cell culture

133 Human iPSC lines were maintained on a feeder-free culture system. The 6-well plates were  
134 pre-coated with Geltrex, LDEV-free hESC qualified reduced growth factor basement  
135 membrane matrix (Invitrogen, A1413302). Geltrex was thawed overnight at 4°C and diluted  
136 1:100 in KO-DMEM medium (Invitrogen, 10829018). Each well was coated with 1.5 ml  
137 Geltrex, incubated for one hour at 37°C, and was then replaced with the mTeSR1 medium  
138 (StemCell Technologies, 05850) with 10 ng/ml bFGF at 37°C and 5% CO<sub>2</sub>. iPSCs were cut  
139 and paste into Geltrex-coated wells. The medium was renewed daily and passaged every 6  
140 days. Then, chemicals such as Rapamycin were added to respective experiments.

141 For induction of autophagy signaling, iPSC colonies were cultured in mTeSR1 medium  
142 supplemented with 0-300 nM Rapamycin (Sigma, R8781) for 1-9 days. For autophagic flux  
143 assay, human iPSCs were treated with 200 nM Rapamycin in the absence or presence of 50

144 nM Bafilomycin A1 for 24 hrs (Sigma, B1793) as specified. Cells were collected and protein  
1  
2 was subsequently analyzed by immunoblotting.  
3

#### 6 146 **EB formation by cut-and-paste method**

7  
8  
9 147 The cut-and-paste method was deployed to make conventional EBs as iPSCs. Spontaneously  
10  
11 148 differentiated cells were removed under a stereomicroscope inside the culture safety cabinet,  
12  
13  
14 149 and fresh medium was added to the remaining iPSC colonies, which were cut into small  
15  
16 150 pieces with 10ul pipette tip. The iPSC sections were then scraped off the dish and transferred  
17  
18  
19 151 to a T25 flask in 15ml EB medium (KO DMEM, KO serum, 1X L-glut and 1X NNEA plus  
20  
21 152 50ul beta-mercaptoethanol). The medium was changed every other day, and the EBs were  
22  
23  
24 153 cultured for 7-10 days before plating out for spontaneous differentiation assays.

#### 26 154 **Antibodies and reagents**

27  
28  
29 155 The reagents for TEM include Sodium cacodylate (C0250, Sigma), low viscosity resin kit  
30  
31 156 (AGR1078A, Agar Scientific) and 2 % osmium tetroxide (AGR1016, Agar Scientific), 25 %  
32  
33  
34 157 Glutaraldehyde Solution (23114.02, AMSBIO), and thermanox plastic coverslips (NUNC).  
35  
36 158 For immunocytochemistry, following antibodies were used: anti-LAMP1 (25630), anti-  
37  
38  
39 159 Syntaxin-6 (12370), and anti-NESTIN (105389) from Abcam; SelectFX® Alexa Fluor® 488  
40  
41 160 Endoplasmic Reticulum labeling kit (S34200) from Life Technologies; anti-LC3B from  
42  
43  
44 161 autophagy antibody sampler kit (4445), Alexa Fluor® 488 Goat Anti-Rabbit IgG fluorescent  
45  
46 162 dye (4412), and Alexa Fluor® 555 Goat Anti-Mouse IgG fluorescent dye (4409) from Cell  
47  
48  
49 163 Signaling Technology. For immunoblot experiments, reagents included anti- $\alpha$ -fetoprotein  
50  
51 164 (A8452), anti- $\alpha$ -smooth muscle actin (A2547), anti-ATG13 (SAB3500502) and ATG101  
52  
53 165 (SAB3500503) from Sigma; anti- $\beta$ III tubulin (G7121) from Promega Corporation; anti-  
54  
55  
56 166 ULK2 (56736) from Abcam; anti-LC3B, anti-BECLIN-1, anti-ATG5 from Cell Signalling  
57  
58  
59 167 Technology (D1G9; #8540P, 1:1000) anti-ATG12, and anti-ATG3 from autophagy antibody  
60  
61  
62  
63  
64  
65

168 sampler kit (4445), anti-p-ULK1(Ser317, 6887), anti p-p70 S6K (Thr389, 9205), anti- $\beta$ -Actin  
169 (4967), HRP-conjugated anti-mouse IgG antibody (7076) and HRP-conjugated anti-rabbit-  
170 IgG antibody (7074) from Cell Signaling Technology. MitoGreen (a Green-fluorescent  
171 mitochondrial dye) was purchased from Promokine (PK-CA707-70054).

## 172 **Transmission electron microscopy (TEM)**

173 iPSCs were cultured on Thermanox coverslips in 6-well plates coated with Geltrex, rinsed with  
174 prewarmed (37°C) 0.1M cacodylate buffer, fixed with 2% Glutaraldehyde and 2%  
175 Paraformaldehyde in 0.1M cacodylate buffer for 3 hours at room temperature, rinsed again with  
176 cacodylate buffer and post-fixed with 1% osmium tetroxide in cacodylate for 1hr at room  
177 temperature. Samples were then rinsed with cacodylate buffer, dehydrated through a series of  
178 graded ethanol, embedded in low viscosity resin according to the standard protocol, and  
179 polymerized at 60°C for 48hrs. Ultra-thin sections were obtained using a diamond knife, on a  
180 Leica Reichert Jung ultra-microtome, and stained with the contrasting agents, uranyl acetate and  
181 lead citrate, in a Leica EM AC20 stainer. Sections were examined with a Hitachi H7000  
182 transmission electron microscope fitted with a 1K Hamamatsu Digital Camera and images were  
183 captured using AMTV542 Image Capture Engine software.

## 184 **Immunocytochemistry**

185 To investigate the effect of Rapamycin, iPSC colonies or the embryoid body-like spheres were  
186 transferred to  $\mu$ -Slide 8-well glass bottom (ibidi GmbH, 80826) coated with Geltrex. Cells were  
187 fixed with 4% paraformaldehyde for 10 min at room temperature and washed with PBS 3 times  
188 before permeabilization using 0.5% Triton X-100 for 10 min. Non-specific binding was blocked  
189 with 5% normal goat serum in PBS containing 0.5% Triton X for 1hr prior to incubation with  
190 primary antibodies overnight at 4°C. The wells were washed three times with PBS and incubated  
191 with secondary antibodies for 1hr at room temperature. The nuclei were visualized by Hoechst  
192 counterstaining for 10 min. After washing with PBS, the immunofluorescence was visualized with

193 the Andor Revolution spinning disk confocal microscope, using Andor IQ2 software. The  
194 samples were imaged using a combination of  $\lambda$ 405nm,  $\lambda$ 488nm and  $\lambda$ 564nm lasers.

## 195 **Immunoblotting**

196 Following experimental treatments, cell pellets were resuspended in NP40 cell lysis buffer  
197 (Invitrogen, FNN0021) supplemented with protease inhibitor cocktail (Sigma, P2714). Lysate  
198 was then centrifuged at 13,000 rpm for 10 min at 4°C, and the supernatant was collected and  
199 used for immunoblotting. Protein concentration was determined and the samples were denatured  
200 in sample buffer (62.5 mM Tris-HCl pH 6.8, 2% SDS, 10% glycerol, 2% mercaptoethanol and  
201 0.01% bromophenol blue) at 95°C for 5 min. Proteins were resolved on 10-15% SDS-PAGE  
202 gels and then electrophoretically transferred to a polyvinylidene difluoride (PVDF) membrane  
203 (Bio-Rad, 162-0177). The transfer efficiency was checked by Ponceau-S red staining (Sigma,  
204 P7170). The membranes were washed with Tris-buffered saline containing 0.1% Tween-20  
205 (TBST) for 5 min, incubated in blocking buffer for 1hr at room temperature and incubated  
206 overnight at 4°C with primary antibodies. They were then washed three times for 5 min each  
207 with TBST, incubated with secondary antibodies for 1hr at room temperature and washed in  
208 TBST. Finally, the membranes were visualized by enhanced chemiluminescence using ECL™  
209 Prime (Amersham Biosciences, GZ28980926). The immunoblot band densities were normalized  
210 with its unphosphorylated protein or Actin or GAPDH, and quantified using a densitometer in  
211 the Scion image analysis program (National Institutes of Health, Bethesda, MD, USA).

## 212 **Data analysis and statistical methods**

213 Data were expressed as the mean  $\pm$  SEM or mean  $\pm$  SD as indicated. Significance was assessed  
214 using one-way analysis of variance (ANOVA) followed by the Tukey-Kramer test using  
215 GraphPad Prism version 5.  $p < 0.05$  was considered significant (\*),  $p < 0.01$  very significant (\*\*).

## 216 **Mass spectrometry analysis**

1  
2  
3  
4  
5  
6  
7  
8  
9  
10  
11  
12  
13  
14  
15  
16  
17  
18  
19  
20  
21  
22  
23  
24  
25  
26  
27  
28  
29  
30  
31  
32  
33  
34  
35  
36  
37  
38  
39  
40  
41  
42  
43  
44  
45  
46  
47  
48  
49  
50  
51  
52  
53  
54  
55  
56  
57  
58  
59  
60  
61  
62  
63  
64  
65

217 The iPSCs were lysed in 1% SDS and the lysates were processed by using the FASP protocol as  
218 previously published [19]. Briefly, the cell lysates were sonicated, detergents removed by  
219 sequential washes in spin columns and proteins digested with trypsin. The peptides were  
220 analyzed on Q-Exactive Mass Spectrometer as previously described [20]. The proteins were  
221 identified and quantified with the MaxQuant 1.5 software suite by searching against the human  
222 uniprot database, with N-terminal acetylation and methionine oxidation as variable modification  
223 and a FDR of 0.01. Mass accuracy was set a 4.5 ppm for the MS and 20 ppm for the MS/MS.  
224 LFQ was performed by MaxLFQ as described [21]. One-way ANOVA was carried out to  
225 compare Rapamycin treated samples with control iPSCs. The mean expression levels (M) and  
226 standard error of means (SEM) were quantified, and folds of changes in the treated samples were  
227 calculated against the control iPSCs (set as 1).  $p < 0.05$  was considered statistically significant. A  
228 total of 220 proteins which were significantly altered after Rapamycin treatment were analyzed  
229 by the STRING program for pathway using GO Biological processes and GO cellular  
230 components.

## 232 **Results**

### 233 **Autophagy is a prominent feature of reprogramming cells and stable iPSCs**

234 The autophagy-lysosome and ubiquitin-proteasome systems are the two major pathways that  
235 cells employ to selectively target long-lived and misfolded proteins, protein aggregates, damaged  
236 mitochondria, or unwanted cytoplasmic components and organelles [22]. We **observed** large  
237 autophagic vacuoles **in the majority of cells** during early reprogramming (red arrowheads, Figure  
238 1A). In young passages of stable iPSCs, autophagic vacuoles were abundantly present but  
239 reduced in size (red arrowheads, Figure 1B). **However, large autophagic vacuoles were absent in**  
240 **parental fibroblasts (Figure 1F).** TEM revealed the presence of lysosomal structures (blue  
241 arrowheads, Figure 1E,I) in iPSCs. Structures of endosomal/lysosomal nature with double



242 membranes were clearly evident under high magnification, which were filled with an array of  
243 cell debris and organelles (Figure 1J-L).

244 Double immunofluorescence staining was carried out with anti-LC3B (an autophagy marker) and  
245 anti-LAMP1 (a major component of lysosomal membrane). In fibroblasts, fine dots of LC3B  
246 staining (green, Figure 1G) were observed and most of them were not colocalized with LAMP1  
247 (red, Figure 1G). Similar to fibroblasts, small dots of LC3B staining were observed in iPSC  
248 culture which were not co-localized with LAMP1. However, strong LC3B staining appeared in  
249 large vacuoles (green, Figure 1C) which co-localized with anti-LAMP1 staining, which could  
250 represent different status of LC3B activity. The control double staining were performed with  
251 anti-Syntaxin 6, a marker for Golgi membrane and MitoGreen for mitochondria (Figure 1D,H).  
252 As anticipated, they were no colocalization in either iPSCs (Figure 1D) or fibroblasts (Figure  
253 1H). These data therefore demonstrate that large autophagic vacuoles are a characteristic feature  
254 of iPSCs which harbor both LC3B-II and LAMP1.

### 255 **iPSCs exhibit higher abundance of LC3B-II than parental fibroblasts**

256 Next we compared iPSCs with parental fibroblasts from 4 independent donors by both  
257 immunocytochemistry (Figure 2a-D') and immunoblotting (Figure 2E-G). The immunofluorescence  
258 study showed brighter basal LC3B-II staining in iPSCs (Figure 2A-D) than in parental  
259 fibroblasts (Figure 2a-d). Rapamycin (100nM) induced autophagy in both iPSCs (Figure 2A'-D')  
260 and fibroblasts (Figure 2a'-d'). Quantification of the immunoblots (Figure 2E) showed 2.55-fold  
261 higher basal LC3B-II in the iPSCs than that in parental fibroblasts (Figure 2F,  $p < 0.01$ ,  $n = 4$ ).  
262 After one day of Rapamycin induction at 100 nM, the LC3B-II was also 2.23-fold higher in the  
263 iPSCs than in fibroblasts (Figure 2G,  $p < 0.05$ ,  $n = 4$ ). Overall, these data show that autophagy is  
264 highly active in human iPSCs and is Rapamycin-inducible. Both the basal and induced  
265 autophagy are significantly higher in iPSCs than in dermal fibroblasts.

266 **High basal levels of autophagy components are expressed in iPSCs**

1  
2  
3 267 To further address the autophagy activity during iPSC maintenance, we determined basal  
4  
5 268 expression levels of 10 autophagy members involving different steps of autophagy. Autophagy is  
6  
7  
8 269 repressed by the mTOR and activated by Rapamycin. ULK1/2 are activated in a ULK1/2-  
9  
10 270 Atg13/101-FIP200 complex [23-24], which subsequently activates PI3K CIII complex  
11  
12 271 (consisting of BECLIN-1, AMBRA, VPS34/15 and ATG14) and stimulates phagophore  
13  
14 272 formation. ATG12 then conjugates with ATG5/16 and form phagophore [25]. ATG4/7/3 then  
15  
16 273 converts LC3B-I to LC3B-II to form autophagic vacuole [17,22,26-27]. We extracted proteins  
17  
18 274 from 12 iPSC lines derived from 10 independent donors (Figure 3), and carried out  
19  
20 275 immunoblotting with antibodies against AMPK $\alpha$ , ULK1, ULK2, ATG13, ATG101, BECLIN-1,  
21  
22 276 ATG3, ATG5, ATG12 and LC3B. Relative protein abundance was quantified against house-  
23  
24 277 keeping proteins. AMPK $\alpha$ , BECLIN-1 ATG12, ATG13 and ULK1 were shown to be highly  
25  
26 278 expressed in iPSCs, whereas ATG3, ATG101 and ULK2 were less abundant. No significant  
27  
28 279 difference was detected among different lines for each component, but high levels of LC3B-II  
29  
30 280 were detected in all iPSCs line (Figure 3A and 3C). To further evaluate the difference between  
31  
32 281 iPSCs and fibroblasts, we investigated ATG5 and ATG12 expression among three fibroblast  
33  
34 282 lines and 5 iPSC lines. The iPSCs were consistently showed to have much higher ATG5/ATG12  
35  
36 283 expression compared to fibroblasts (Figure 3H). These data demonstrate that most autophagy  
37  
38 284 components are abundantly expressed in iPSCs.  
39  
40  
41  
42  
43  
44  
45  
46

47 **Rapamycin induces iPSC autophagy in concentration- and time-dependent manners**

48  
49  
50  
51 286 To determine if iPSC maintenance might benefit from upregulated autophagy, we investigated  
52  
53 287 the dosage effect of Rapamycin on phosphorylated ULK1, p70S6K, and the autophagy indicator  
54  
55 288 - ratio of LC3B-II/I. Both ULK1 and p70S6K are serine/threonine kinases and targets of mTOR.  
56  
57  
58  
59  
60  
61  
62  
63  
64  
65

1  
2  
3  
4  
5  
6  
7  
8  
9  
10  
11  
12  
13  
14  
15  
16  
17  
18  
19  
20  
21  
22  
23  
24  
25  
26  
27  
28  
29  
30  
31  
32  
33  
34  
35  
36  
37  
38  
39  
40  
41  
42  
43  
44  
45  
46  
47  
48  
49  
50  
51  
52  
53  
54  
55  
56  
57  
58  
59  
60  
61  
62  
63  
64  
65

289 p70S6K is a major regulator of translation and phosphorylated by mTOR [28-30], whereas  
290 ULK1 is an initiator of autophagy.

291 We treated iPSCs with 0, 1, 10, 100, 200 or 300 nM of Rapamycin for 4 days, and observed a  
292 dose-dependent reduction in p70S6K phosphorylation (Figure 4I). The most significant reduction  
293 was achieved with 100-300 nM (Figure 4K). In contrast, LC3B-II (Figure 4J) and p-ULK1  
294 (Figure 4L) were enhanced in a dose-dependent manner, and the maximal increase was observed  
295 at 200 nM of Rapamycin ( $p<0.01$ ). Similarly, immunostaining detected higher levels of LC3B-II  
296 expression in 200 nM Rapamycin-induced cells (Figure 4A-D).

297 We then treated iPSCs with 200 nM of Rapamycin for 1, 3 and 6 days, observed significantly  
298 clustered LC3B-II staining after 3 days of Rapamycin treatment, and showed a time course-  
299 dependent activation of autophagy (Figure 4E-H). This was different from fibroblasts, in which  
300 the total LC3B was increased by 24 hrs of Rapamycin treatment, whereas the LC3B-II remained  
301 relatively constant (supplement Figure 1). These data demonstrate that autophagy can be  
302 markedly activated by Rapamycin in iPSCs.

### 303 **Rapamycin attenuates Bafilomycin-induced iPSC death**

304 Bafilomycin A1 is an inhibitor of lysosome degradation by blocking the final stage of  
305 autophagy, fusion of autophagosomes with lysosome (31-32). We treated iPSCs with 0, 5, 50,  
306 100 nM of bafilomycin A1 for 24 or 48 hrs, with or without 200nM Rapamycin. Bafilomycin  
307 A1 was shown to induce iPSC death in concentration/time dependent manners. iPSC  
308 morphology was significantly altered after 24 hr of Bafilomycin treatment at 50 nM (Figure  
309 5) but not at 5 nM (Figure 5B). At 100 nM, Bafilomycin markedly induced iPSC death in 24  
310 hrs, leading to grossly reduced cell density after 48 hrs (Figure 5E). Addition of 200 nM  
311 Rapamycin significantly attenuated Bafilomycin-induced cell death, improved iPSC survival  
312 and increased iPSC cell density at 48 hrs Bafilomycin treatment (Figure 5G).

1  
2  
3  
4  
5  
6  
7  
8  
9  
10  
11  
12  
13  
14  
15  
16  
17  
18  
19  
20  
21  
22  
23  
24  
25  
26  
27  
28  
29  
30  
31  
32  
33  
34  
35  
36  
37  
38  
39  
40  
41  
42  
43  
44  
45  
46  
47  
48  
49  
50  
51  
52  
53  
54  
55  
56  
57  
58  
59  
60  
61  
62  
63  
64  
65

313 Western blotting showed that Bafilomycin enhanced both LC3B-I and -II bands by blocking  
314 basal autophagic flux. Rapamycin induced LC3B expression and caused a shift from LC3B-I  
315 to the LC3B-II (Figure 5H-I). Treatment of iPSCs with both Rapamycin and bafilomycin A1  
316 increased conversion of LC3B-II from LC3B-I similar to Rapamycin treatment alone, thereby  
317 attenuated bafilomycin-induced cell death (Figure 5C-D). These data further strengthen the  
318 importance of autophagy in iPSCs, as blockage of fusion of autophagosomes with lysosome  
319 rapidly induces iPSC death. Meanwhile addition of Rapamycin significantly improves the  
320 iPSC survival.

### 321 **Prolonged treatment with Rapamycin induces formation of uniform aggregates**

322 We next cultured iPSCs in geltrex-coated dishes in the presence of 200 nM of Rapamycin and  
323 examined the long-term effects on the maintenance of iPSCs. We first noticed the following  
324 morphological changes: (1) the peripheral cells of the iPSC colonies first started to elongate  
325 (Figure 6D) after 3 days, and cells at the edge produced an unknown matrix which formed a firm  
326 line at the border of colony after 6 days to limit iPSC colony expansion sideways (arrowheads,  
327 Figure 6F-G); (2) Rapamycin altered iPSC cell junctions, and cell borders became more obvious  
328 after 2 days of treatment (Figure 6C-D); and (3) iPSCs continued to proliferate in the central  
329 areas of colonies, together with the limitation to expand sideways and reduced cell-cell contacts,  
330 round EB-like spheres were formed and detached from the culture dish before and after 6 days of  
331 Rapamycin treatment (\*, Figure 6E-F).

332 The average aggregate size at 6 days was  $64793 \pm 18779 \mu\text{m}^2$  (n=13). The round spheres  
333 continued to detach and grow after 9 days of treatment, and reached the sizes of  $112251 \pm 17422$   
334  $(002V, n=8)$ ,  $104640 \pm 27265$  (JOM, n=13),  $105381 \pm 13468 \mu\text{m}^2$  (LV1, n=7) in three independent  
335 iPSC lines, respectively. However, the control EBs resulted from the cut-and-paste method  
336 varied significantly in shape and sizes (Figure 7F-H). They were  $52328 \pm 25518$  (002V, n=10);  
337  $80518 \pm 77708$  (JOM, n=20);  $75652 \pm 51944 \mu\text{m}^2$  (LV1, n=22), respectively, and displayed

338 consistently large variation (SD) in sizes within each line (Figure 7B). These data show that high  
339 concentrations of Rapamycin treatment can induce iPSC detachment and spontaneous formation  
340 of uniformly sized aggregates.

### 341 **Rapamycin treatment accelerates differentiation of human iPSCs**

342 To determine the nature of the floating spheres resulting from Rapamycin treatment, we  
343 extracted proteins from the aggregates and compared them with EBs generated *via* the cut-and-  
344 paste method by immunoblotting with three germ layer markers of  $\alpha$ -fetoprotein (AFP for  
345 endoderm),  $\alpha$ -smooth muscle actin (ASM for mesoderm), and  $\beta$ III tubulin (TUJ1 for ectoderm),  
346 together with autophagy marker LC3B-II (Figure 8A). The expression of these marker proteins  
347 was 2~3 fold higher in the Rapamycin-induced spheres (Figure 8A-C).

348 To examine differentiation potential of aggregates, we plated them out for spontaneous  
349 differentiation and compared with EBs made mechanically. Cells with neuronal morphology  
350 appeared after 3 days without neuronal induction (Figure 8J-L), and many were stained positive  
351 for neural stem cell marker NESTIN (Figure 8M). After 5 days of spontaneous differentiation,  
352 we carried out immunocytochemical staining with AFP, ASM, TUJ1, and obtained significantly  
353 higher proportions of cells positive for these makers in cells derived from Rapamycin-induced  
354 spheres (Figure 8G-I), compared with cells differentiated from the conventional EBs (Figure 8D-  
355 F). To illustrate mechanism(s) of Rapamycin-induced iPSC differentiation, we investigated  
356 NANOG expression after 4 days of treatment by immunoblotting (Figure 8L). Rapamycin was  
357 shown to down-regulate NANOG expression in a concentration-dependent manner, and  
358 significant reductions were detected at 100 nM ( $p < 0.05$ ), 200 nM ( $p < 0.01$ ) or 300 nM of  
359 Rapamycin treatment ( $p < 0.01$ , Figure 8M). These data suggest that Rapamycin-induced spheres  
360 are similar to conventional EBs in pluripotency of differentiation, they are non-biased in

1  
2  
3  
4  
5  
6  
7  
8  
9  
10  
11  
12  
13  
14  
15  
16  
17  
18  
19  
20  
21  
22  
23  
24  
25  
26  
27  
28  
29  
30  
31  
32  
33  
34  
35  
36  
37  
38  
39  
40  
41  
42  
43  
44  
45  
46  
47  
48  
49  
50  
51  
52  
53  
54  
55  
56  
57  
58  
59  
60  
61  
62  
63  
64  
65

361 differentiating into three lineages, but differentiate in an accelerated pace, in association with  
362 down-regulated NANOG expression during EB formation.

### 363 **Rapamycin regulates adherens junctions and actin cytoskeleton in human iPSCs**

364 To identify potential molecular mechanisms associated with Rapamycin-induced iPSC  
365 detachment, we performed quantitative mass spectrometry analysis with proteins extracts from  
366 control iPSCs and iPSCs treated with 50, or 100 nM of Rapamycin for 3, 6, 9 days respectively  
367 (n=3 for each). A total of 6145 proteins were quantitatively identified, and 220 proteins were  
368 identified by statistical analyses, which were systematically altered at different time points and at  
369 both Rapamycin concentrations (One-way ANOVA, two-tailed,  $p<0.05$ ). Gene ontology (GO)  
370 analyses of the 220 targets with the STRING database revealed that adherens junctions (17 hits,  
371  $p=6.49\times 10^{-6}$ ) and actin cytoskeleton (9 hits,  $p=0.022$ ) were significantly enriched in the  
372 Rapamycin-treated cells (Figure 9), which integrated into an interactive network (Figure 9F).

373 Of the 17 adherens junction molecules, 9 (ACTN4, BSG, EPHA2, EZR, FLNB, PDLIM1, PPIA,  
374 SHROOM3, RPLP0) were down-regulated, and 8 (ABI2, GSN, ACTR3, ARF6, RALA, RPL7A,  
375 RPL19, RPL27) were up-regulated (Figure 9A-C). Of the 9 actin cytoskeleton associated  
376 proteins, 6 (ACTN4, CGN, EZR, FGD4, SERPINA3, TTN) were down-regulated and 3  
377 (CTTNBP2NL, GSN, SEPT11) were up-regulated (Figure 9D-E). In consistent with the  
378 morphological changes, these data suggest that alterations of adherens junctions and  
379 cytoskeleton are the key pathways in Rapamycin-induced iPSC behavior.

### 381 **Discussion**

382 Autophagy is a cellular mechanism to maintain minimal cell activity for viability in response to  
383 nutrient limitations and cell stress, by degrading and recycling cytoplasmic proteins and

384 subcellular organelles *via* the fusion of a double-membrane-bound vesicle, autophagosome, with  
1  
2  
3 385 lysosome [17,33]. Autophagy plays an essential role in cellular reprogramming and basal level of  
4  
5 386 autophagy increases in aging human skin fibroblasts, which may affect to different  
6  
7 387 reprogramming efficiency [34]. It appears there is no co-relation with sex (all male) or age (4-  
8  
9 388 20-year) in the fibroblast lines we have used, but with health status, which requires validation in  
10  
11 389 larger sample sets. In this study we demonstrate abundant presence of large autophagic vacuoles  
12  
13 390 in early fibroblast reprogramming and smaller ones during the iPSC maintenance. We show high  
14  
15 391 basal level of key components of autophagy in 12 iPSC lines derived from 10 independent  
16  
17 392 donors, and prolonged Rapamycin treatment resulted spontaneous formation of uniform sized  
18  
19 393 EBs with accelerated differentiation pace.

20  
21  
22  
23  
24  
25 394 In previous studies, lack of autophagy components of Atg3, or Atg5 or Atg7 was shown to  
26  
27 395 render MEF cells defective in iPSC colony formation [15], and lack of two different autophagy  
28  
29 396 genes, *atg5* and *beclin1*, displayed a defect in EB formation during development [35]. The  
30  
31 397 reprogramming was entirely blocked also in *Tsc2*<sup>-/-</sup> somatic cells with hyperactivated mTOR  
32  
33 398 activity which suppressed autophagy [14]. Subtle tuning of the mTOR activity with inhibitors,  
34  
35 399 i.e. 0.3-1 nM Rapamycin or 0.1 nM PP242 was found to increase reprogramming efficiency [18].  
36  
37 400 Mechanistically, the reprogramming factor Sox2 could bind to mTOR promoter and repress  
38  
39 401 mTOR expression and activate autophagy [15]. These data together showed that reduced mTOR  
40  
41 402 activity and elevated Autophagy were required during cellular reprogramming, which is  
42  
43 403 consistent with our observation that abundant large autophagic vacuoles are present in early  
44  
45 404 fibroblast reprogramming, which become smaller during the subsequent passaging.

46  
47  
48  
49  
50  
51  
52 405 A balanced autophagy and mTOR activity is also essential for the maintenance and  
53  
54 406 differentiation of pluripotent stem cells. Human ES cells were previously shown to have a tight  
55  
56 407 regulation of the mTOR signaling to mediate protein translation for maintaining the pluripotent  
57  
58 408 status [36]. Activation of p70S6K, a mTOR downstream factor, was shown to induce  
59  
60  
61  
62  
63  
64  
65



1  
2  
3  
4  
5  
6  
7  
8  
9  
10  
11  
12  
13  
14  
15  
16  
17  
18  
19  
20  
21  
22  
23  
24  
25  
26  
27  
28  
29  
30  
31  
32  
33  
34  
35  
36  
37  
38  
39  
40  
41  
42  
43  
44  
45  
46  
47  
48  
49  
50  
51  
52  
53  
54  
55  
56  
57  
58  
59  
60  
61  
62  
63  
64  
65

409 differentiation of human ES cells [36], whereas inhibition of mTOR autophosphorylation by 20  
410 nM Rapamycin was reported to disrupt p70S6K-mediated translation, but not to alter cell  
411 viability or expression of the pluripotency markers [37]. In contrast, the mTOR was necessary  
412 for growth and proliferation of early mouse embryos and ES cells, and disruption of the mouse  
413 mTOR gene prohibited ES cell development [38-39]. **Interestingly, 100nM Rapamycin was**  
414 **previously shown to reduce the size and rate of EB formation in human amniotic fluid stem cells**  
415 **[40]. This was different from our study that high concentration of Rapamycin induced EB**  
416 **formation in iPSCs.** Inhibition of the mTOR activity with high concentrations of Rapamycin also  
417 greatly impaired somatic cell reprogramming [14], and 100 nM Rapamycin was used to primer  
418 hepatocyte differentiation of iPSCs prior to Activin A induction [41]. **This is consistent with our**  
419 **data that Rapamycin down-regulates NANOG expression in a concentration dependent manner**  
420 **and accelerates iPSC differentiation.**

421 To uncover Rapamycin pathways in iPSCs, we carried out quantitative mass spectrometry. The  
422 STRING Gene Ontology analyses revealed that actin cytoskeleton and adherens junctions were  
423 the integrated pathways regulated by Rapamycin. For example, ACTN4, BSG, CGN, EPHA2,  
424 EZR, FGD4, FLNB, PDLIM1, PPIA, SHROOM3, RPLP0, SERPINA3 and TTN were  
425 significantly down-regulated, whereas ABI2, CTTNBP2NL, GSN, ACTR3, ARF6, RALA,  
426 RPL7A, RPL19, RPL27 and SEPT11 were up-regulated.

427 Actin is critical for cell shape, adhesion and migration. The dynamics of actin cytoskeleton are  
428 modulated by Rapamycin targets of SHROOM3, EZR and GSN. For example, SHROOM3 is  
429 required for the apical localization of F-actin/myosin II [42]. EZR links the plasma membrane to  
430 actin and is involved in adhesion and migration. Inhibition of EZR expression reduced  
431 adhesiveness in colorectal cancer cells [43]. GSN knockdown decreased cell viability and tumor  
432 cell invasion, whereas GSN overexpression correlates with proliferative and invasive capacities  
433 [44]. BSG promotes cell–cell adhesion, and its down-regulation altered actin/Spectrin network

1  
2  
3  
4  
5  
6  
7  
8  
9  
10  
11  
12  
13  
14  
15  
16  
17  
18  
19  
20  
21  
22  
23  
24  
25  
26  
27  
28  
29  
30  
31  
32  
33  
34  
35  
36  
37  
38  
39  
40  
41  
42  
43  
44  
45  
46  
47  
48  
49  
50  
51  
52  
53  
54  
55  
56  
57  
58  
59  
60  
61  
62  
63  
64  
65

434 [45]. Therefore, reduced expression of SHROOM3, EZR and BSG in the Rapamycin-treated  
435 iPSCs is in line with reduced cell adhesion in the literature.

436 ACTN4, FLNB, PDLIM1 are actin-binding proteins. ACTN4 is concentrated at sharp extension  
437 and at the edge of cell clusters [46], and FLNB regulates direct communication between the cell  
438 membrane and cytoskeletal network [47]. PDLIM1 function as an adapter to recruit other LIM-  
439 interacting proteins to the cytoskeleton, and suppression of PDLIM1 resulted in cell spreading  
440 and the loss of stress fibers and focal adhesions [48]. In addition, ACTR3 is also essential to cell  
441 shape and motility, and is an ATP-binding component of the ARP2/3 complex, which regulates  
442 actin polymerization. The complex can be activated by ABI, and knockdown of ABI markedly  
443 inhibits cell-cell junctions [49]. Therefore, Rapamycin-induced changes in the expression of  
444 ACTN4, ACTR3, FLNB and PDLIM1 are also likely to affect actin cytoskeleton.

445 Some of Rapamycin targets are GTPase activity-related, such as downregulated EPHA2 and  
446 upregulated ARF6 and RALA. GTPases are involved in cell adhesion migration and oncogenic  
447 transformation. For example, EphA2 is a transmembrane receptor tyrosine kinase activating and  
448 prompts cells to round up and detach from their neighbors [50]. RALA is a small GTPase and  
449 constitutively active RALA promotes anchorage-independent growth signaling [51]. ARF6 is a  
450 small GTPase to balance with RAB35 GTPase by cells during cell migration and adhesion.  
451 Increased ARF6 activity from RAB35 knockdown enhances cadherins accumulation and reduces  
452 cell–cell adhesion. The loss of RAB35, However, correlates with enhanced cell migration [52].  
453 Therefore, reduced EPHA2 and increased ARF6 and RALA expression may also contribute to  
454 Rapamycin-induced iPSC detachment. Together these data showed that Rapamycin regulates an  
455 array of adherens junctions and actin modifying molecules, which collectively alters iPSC  
456 adhesion.

457

1  
2  
3 458 **Conclusions**

4  
5 459 In this study, we demonstrate that autophagy is a prominent feature of reprogramming cells  
6  
7 460 and stable iPSCs. The basal level of autophagy is universally present among human iPSC  
8  
9 461 lines, which is significantly higher than parental fibroblasts. **Block of autophagy by**  
10  
11 462 **Bafilomycin induces iPSC death.** Rapamycin activates autophagy in concentration- and time-  
12  
13 463 dependent manners **and attenuate Bafilomycin toxicity** in iPSCs. Prolonged Rapamycin  
14  
15 464 treatment induces cell detachment and formation of uniformly sized EBs from human iPSCs,  
16  
17 465 with altered expression of adherens junctions and actin modifying molecules. The Rapamycin  
18  
19 466 downregulates NANOG expression, induces EBs formation and accelerates cell  
20  
21 467 differentiation into three germ layer lineages. This findings are significant in two-fold.  
22  
23 468 Firstly, the 3D microenvironment including shape and sizes of EBs can affect differentiation.  
24  
25 469 The iPSCs are supersensitive to enzyme dissociation and therefore the “hanging drop”  
26  
27 470 technique is difficult to apply, despite it was available to generate uniform EBs from ES cells  
28  
29 471 over 20 years ago. Rapamycin may therefore assist generation of uniformly sized EB with  
30  
31 472 round shape which may reduce the heterogeneity of the end cell types. Secondly,  
32  
33 473 differentiation of mature and functional cell types from human iPSCs is time-consuming, and  
34  
35 474 the accelerated differentiation associated with Rapamycin treatment is promising in  
36  
37 475 shortening the differentiation duration. Rapamycin, therefore, may find its application in  
38  
39 476 assistance of overcoming the challenges associated with phenotypic characterization, drug  
40  
41 477 discovery and cell replacement therapy for neurological disorders.  
42  
43  
44  
45  
46  
47  
48  
49  
50  
51  
52  
53

54 478  
55  
56  
57 479 **Declarations**

58 480 **Abbreviations**  
59  
60  
61  
62  
63  
64  
65

1 481 AFP,  $\alpha$ -fetoprotein; ANOVA, one-way analysis of variance; ASM,  $\alpha$ -smooth muscle actin;  
2 482 ATGs, Autophagy-Related Genes; EBs, embryoid bodies; ER, endoplasmic reticulum; ES,  
3 embryonic stem; iPSCs, induced pluripotent stem cells; LC3I, microtubule-associated  
4 483 proteins 1A/1B light chain 3-I; MEF, mouse embryonic fibroblasts; mTOR, mammalian  
5 484 target of the Rapamycin; NaB, sodium butyrate; PE, phosphatidylethanolamine; PVDF,  
6 polyvinylidene difluoride; SEM, standard error of means; TEM, transmission electron  
7 485 microscopy; TUJ1,  $\beta$ III tubulin.

### 18 488 **Ethical approval and consent to participate**

21 489 The iPSC study was carried out in compliance with the ethical approval of the Clinical Research  
22 Ethics Committee, Galway University Hospitals, and informed consent was obtained from all  
23 490 participants prior to skin biopsy donation.

### 30 492 **Consent for publication**

33 493 Informed consent was obtained from volunteers for disclosure of the research data  
34 494 anonymously.

### 39 495 **Availability of supporting data**

43 496 Not applicable.

### 46 497 **Competing interests**

50 498 Authors declare no potential conflicts of interest.

### 53 499 **Funding**

1 This work was supported by Science Foundation Ireland (SFI), Strategic Research Cluster  
2 (SRC), grant No. SFI: 09/SRC B1794 and 09/SRC/B1794s1, SFI Investigator Programme  
3  
4 502 13/IA/1787, SFI TIDA program 14/TIDA/2258; NUI Galway Grant RSU002.  
5  
6  
7

### 8 **Authors' contributions**

9

10  
11 504 A.S. performed the majority of the experiments; K.M. and A.K made iPSC lines, K.M.  
12  
13 505 contributed IC/WB data during revisions; M.J.D and T.K contributed additional iPSC lines;  
14  
15 506 J.K and V.M in patient recruitment; K.T and P.D participated in microscopic  
16  
17 507 characterization; K.D.C did independent treatment for proteomics, A.v.K and A.G-M  
18  
19 508 performed proteomics; F.B., and T.O oversaw the project and edited manuscript; A.S and S.S  
20  
21 509 designed the experiments, analyzed the data and wrote the manuscript.  
22  
23  
24  
25  
26

### 27 **Acknowledgements**

28

29  
30  
31 511 The authors acknowledge the facilities and technical assistance from the Centre for Microscopy  
32  
33 512 & Imaging at the National University of Ireland Galway ([www.imaging.nuigalway.ie](http://www.imaging.nuigalway.ie)), a facility  
34  
35 513 that is funded by NUIG and the Irish Government's Programme for Research in Third Level  
36  
37 514 Institutions, Cycles 4 and 5, National Development Plan 2007-2013.  
38  
39  
40

### 41 **Authors' information**

42

43  
44  
45 516 A.S: BSc, MSc, PhD, postdoctoral researcher, Regenerative Medicine Institute, School of  
46  
47 517 Medicine, NUI Galway, Ireland, and now a Lecturer at Chulabhorn International College  
48  
49 518 of Medicine, Thammasat University, Thailand.

50  
51  
52 519 K.M.: BSc, MSc, PhD, postdoctoral researcher, Regenerative Medicine Institute, School of  
53  
54 520 Medicine, NUI Galway, Ireland.

55  
56  
57 521 A.v.K.: BSc, MSc, PhD, Research Fellow, Systems Biology Ireland, University College  
58  
59 522 Dublin, Ireland, and now Mass-spectrometry Manager at Edinburgh University, UK.  
60  
61  
62  
63  
64  
65

- 1  
2  
3  
4  
5  
6  
7  
8  
9  
10  
11  
12  
13  
14  
15  
16  
17  
18  
19  
20  
21  
22  
23  
24  
25  
26  
27  
28  
29  
30  
31  
32  
33  
34  
35  
36  
37  
38  
39  
40  
41  
42  
43  
44  
45  
46  
47  
48  
49  
50  
51  
52  
53  
54  
55  
56  
57  
58  
59  
60  
61  
62  
63  
64  
65
- 523 A.G-M.: BSc, MSc, PhD, Lab Manager, Systems Biology Ireland, Conway Institute, UCD,  
Ireland.
- 524
- 525 A.K.: MSc, Regenerative Medicine Institute, School of Medicine, NUI Galway, Ireland.
- 526 K.T.: BSc, PhD, Postdoctor Microscopy Facility Scientist, School of Medicine, NUI Galway,  
Ireland.
- 527
- 528 K.D.C.: MSc, PhD, Postdoctor, Regenerative Medicine Institute, School of Medicine, NUI  
Galway, Ireland.
- 529
- 530 J.K., MB, MD, Consultant Haematologist, Senior Lecturer, Galway University Hospital.
- 531 V.M.: MSc, PhD, Clinical Manager , HRB Clinical Research Facility, NUI Galway, Ireland.
- 532 P.D.: BSc, PhD, Head of Anatomy, Centre for Microscopy and Imaging, School of Medicine,  
NUI Galway, Ireland.
- 533
- 534 M.J.D.: MD, PhD, MRC Clinical Research Fellow at MRC center for Regenerative Medicine,  
The University of Edinburgh, UK.
- 535
- 536 T.K.: BSc, MSc, PhD, Principal Investigator, MRC center for Regenerative Medicine, The  
University of Edinburgh, UK.
- 537
- 538 F.B., BSc, MSc, PhD, Professor of Cellular Therapy and Scientific Director of the  
Regenerative Medicine Institute, School of Medicine, NUI Galway, Ireland.
- 539
- 540 T.O.: MB BCh BAO , MD, PhD, Director of the Regenerative Medicine Institute, Dean of the  
College of Medicine and Life Sciences, NUI Galway, Ireland.
- 541
- 542 S.S.: BSc, MSc, PhD, Professor of Fundamental Stem Cell Biology, Regenerative Medicine  
Institute, School of Medicine, NUI Galway, Ireland.
- 543

## 544 **References**

- 545
- 546 1. Takahashi K, Yamanaka S. Induction of pluripotent stem cells from mouse embryonic and  
547 adult fibroblast cultures by defined factors. Cell. 2006;126:663-76.
- 548

- 548 2. Chu A, Caldwell JS, Chen YA. Identification and characterization of a small molecule  
1 antagonist of human VPAC(2) receptor. *Mol Pharmacol.* 2010;77:95-101.  
2  
3 549  
4  
5 550 3. Dolmetsch R, Geschwind DH. The human brain in a dish: the promise of iPSC-derived  
6  
7 551 neurons. *Cell.* 2011;145:831-34.  
8  
9  
10 552 4. Bellin M, Marchetto MC, Gage FH, Mummery CL. Induced pluripotent stem cells: the  
11  
12 553 new patient? *Nat Rev Mol Cell Biol.* 2012;13:713-26.  
13  
14 554 5. Chailangkarn T, Acab A, Muotri AR. Modeling neurodevelopmental disorders using  
15  
16 555 human neurons. *Curr Opin Neurobiol.* 2012; 22:785-90.  
17  
18  
19 556 6. Kim KY, Jung YW, Sullivan GJ, Chung L, Park IH. Cellular reprogramming: a novel  
20  
21 557 tool for investigating autism spectrum disorders. *Trends Mol Med.* 2012;18:463-71.  
22  
23  
24 558 7. Nakano T, Ando S, Takata N, Kawada M, Muguruma K, Sekiguchi K, et al. Self-  
25  
26 559 formation of optic cups and storable stratified neural retina from human ESCs. *Cell Stem*  
27  
28 560 *Cell.* 2012;10:771-85.  
29  
30  
31 561 8. Sasai Y, Eiraku M, Suga H. In vitro organogenesis in three dimensions: self-organising  
32  
33 562 stem cells. *Development.* 2012;139:4111-21.  
34  
35  
36 563 9. Lancaster MA, Renner M, Martin CA, Wenzel D, Bicknell LS, Hurles ME, et al.  
37  
38 564 Cerebral organoids model human brain development and microcephaly. *Nature.*  
39  
40 565 2013;501:373-79.  
41  
42  
43 566 10. Hwang YS, Chung BG, Ortmann D, Hattori N, Moeller HC, Khademhosseini A.  
44  
45 567 Microwell-mediated control of embryoid body size regulates embryonic stem cell fate via  
46  
47 568 differential expression of WNT5a and WNT11. *Proc Natl Acad Sci (USA).* 2009;  
48  
49 569 106:16978-83.  
50  
51  
52 570 11. Hu BY, Du ZW, Zhang SC. Differentiation of human oligodendrocytes from pluripotent  
53  
54 571 stem cells. *Nat Protoc.* 2009; 4:1614-22.  
55  
56  
57  
58  
59  
60  
61  
62  
63  
64  
65



- 572 12. Shi Y, Kirwan P, Livesey FJ. Directed differentiation of human pluripotent stem cells to  
1 cerebral cortex neurons and neural networks. *Nat Protoc.* 2012;7:1836-46.  
2 573  
3  
4  
5 574 13. Liu Y, Liu H, Sauvey C, Yao L, Zarnowska ED, Zhang SC. Directed differentiation of  
6  
7 575 forebrain GABA interneurons from human pluripotent stem cells. *Nat Protoc.* 2013;  
8  
9 576 8:1670-79.  
10  
11  
12 577 14. He J, Kang L, Wu T, Zhang J, Wang H, Gao H, et al. An elaborate regulation of  
13  
14 578 Mammalian target of Rapamycin activity is required for somatic cell reprogramming  
15  
16 579 induced by defined transcription factors. *Stem Cells Dev.* 2012;21:2630-41.  
17  
18  
19 580 15. Wang S, Xia P, Ye B, Huang G, Liu J, Fan Z. Transient activation of autophagy via  
20  
21 581 Sox2-mediated suppression of mTOR is an important early step in reprogramming to  
22  
23 582 pluripotency. *Cell Stem Cell.* 2013;13:617-25.  
24  
25  
26 583 16. Ohsumi Y. Molecular dissection of autophagy: two ubiquitin-like systems. *Nat Rev Mol*  
27  
28 584 *Cell Biol.* 2001; 2:211-16.  
29  
30  
31 585 17. Glick D, Barth S, Macleod KF. Autophagy: cellular and molecular mechanisms. *J Pathol.*  
32  
33 586 2010;221:3-12.  
34  
35  
36 587 18. Chen T, Shen L, Yu J, Wan H, Guo A, Chen J, et al. Rapamycin and other longevity-  
37  
38 588 promoting compounds enhance the generation of mouse induced pluripotent stem cells.  
39  
40 589 *Aging Cell.* 2011;10:908-11.  
41  
42  
43 590 19. Wiśniewski JR, Zougman A, Nagaraj N, Mann M. Universal sample preparation method  
44  
45 591 for proteome analysis. *Nat Methods.* 2009; 6:359-62.  
46  
47  
48 592 20. Farrell J, Kelly C, Rauch J, Kida K, García-Muñoz A, Monsefi N, et al. HGF induces  
49  
50 593 epithelial-to-mesenchymal transition by modulating the mammalian hippo/MST2 and  
51  
52 594 ISG15 pathways. *J Proteome Res.* 2014; 13:2874-86.  
53  
54  
55  
56  
57  
58  
59  
60  
61  
62  
63  
64  
65

- 595 21. Cox J, Hein MY, Lubner CA, Paron L, Nagaraj N, Mann M. Accurate proteome-wide  
1 label-free quantification by delayed normalization and maximal peptide ratio extraction,  
2 596 termed MaxLFQ. *Mol Cell Proteomics*. 2014; 13:2513-26.  
3  
4 597  
5  
6  
7 598 22. Nixon RA. The role of autophagy in neurodegenerative disease. *Nat Med*. 2001; 19:983-  
8  
9 599 97.  
10  
11 600 23. Klionsky DJ, Cregg JM, Dunn WJr, Emr SD, Sakai Y, Sandoval IV, et al. A unified  
12  
13 601 nomenclature for yeast autophagy-related genes. *Dev Cell*. 2003; 5:539-45.  
14  
15 602 24. Klionsky DJ. The molecular machinery of autophagy: unanswered questions. *J Cell Sci*.  
16  
17 603 2005; 118:7-18.  
18  
19 604 25. Sakoh-Nakatogawa M, Matoba K, Asai E, Kirisako H, Ishii J, Noda NN, et al. Atg12-  
20  
21 605 Atg5 conjugate enhances E2 activity of Atg3 by rearranging its catalytic site. *Nat Struct*  
22  
23 606 *Mol Biol*. 2013; 20:433-39.  
24  
25  
26 607 26. Jaeger PA, Wyss-Coray T. All-you-can-eat: autophagy in neurodegeneration and  
27  
28 608 neuroprotection. *Mol Neurodegener*. 2009; 4:16.  
29  
30  
31 609 27. Alers S, Löffler AS, Wesselborg S, Stork B. Role of AMPK-mTOR-Ulk1/2 in the  
32  
33 610 regulation of autophagy: cross talk, shortcuts, and feedbacks. *Mol Cell Biol*. 2012; 32:2-  
34  
35 611 11.  
36  
37 612 28. Alessi DR, Kozłowski MT, Weng QP, Morrice N, Avruch J. 3-Phosphoinositide-  
38  
39 613 dependent protein kinase 1 (PDK1) phosphorylates and activates the p70 S6 kinase in  
40  
41 614 vivo and in vitro. *Curr Biol*. 1998; 8:69-81.  
42  
43  
44 615 29. Pullen N, Dennis PB, Andjelkovic M, Dufner A, Kozma SC, Hemmings BA et al.  
45  
46 616 Phosphorylation and activation of p70s6k by PDK1. *Science*. 1998; 279:707-10.  
47  
48  
49 617 30. Weng QP, Kozłowski M, Belham C, Zhang A, Comb MJ, Avruch J. Regulation of the  
50  
51 618 p70 S6 kinase by phosphorylation in vivo. Analysis using site-specific anti-  
52  
53 619 phosphopeptide antibodies. *J Biol Chem*. 1998; 273:16621-29.  
54  
55  
56  
57  
58  
59  
60  
61  
62  
63  
64  
65

- 620 31. Yamamoto A, Tagawa Y, Yoshimori T, Moriyama Y, Masaki R, Tashiro Y.  
1  
2 621 Bafilomycin A<sub>1</sub> prevents maturation of autophagic vacuoles by inhibiting fusion  
3  
4  
5 622 between autophagosomes and lysosomes in rat hepatoma cell line, H-4-II-E cells. *Cell*  
6  
7 623 *Struct Funct.* 1998; 23:33-42.  
8  
9  
10 624 32. Klionsky DJ, Elazar Z, Seglen PO, Rubinsztein DC. Does Bafilomycin A<sub>1</sub> block the  
11  
12 625 fusion of autophagosome with lysosomes? *Autophagy.* 2008; 4:849-50.  
13  
14  
15  
16 626 33. Cecconi F, Levine B. The role of autophagy in mammalian development: cell makeover  
17  
18 627 rather than cell death. *Dev Cell.* 2008; 15:344-57.  
19  
20  
21 628 34. Demirovic D, Nizard C, Rattan SIS. Basal Level of Autophagy Is Increased in Aging  
22  
23 629 Human Skin Fibroblasts In Vitro, but not in old Skin. *PLoS one.* 2015; 10:e0126546.  
24  
25  
26 630 35. Qu X, Zou Z, Sun Q, Luby-Phelps K, Cheng P, Hogan RN, et al. Autophagy gene-  
27  
28 631 dependent clearance of apoptotic cells during embryonic development. *Cell.* 2007;  
29  
30 632 128:931-46.  
31  
32  
33  
34 633 36. Zhou J, Su P, Wang L, Chen J, Zimmermann M, Genbacev O, et al. mTOR supports  
35  
36  
37 634 long-term self-renewal and suppresses mesoderm and endoderm activities of human  
38  
39 635 embryonic stem cells. *Proc Natl Acad Sci (USA).* 2009; 106:7840-45.  
40  
41  
42 636 37. Easley CA<sup>4th</sup>, Ben-Yehudah A, Redinger CJ, Oliver SL, Varum ST, Eisinger VM, et al.  
43  
44 637 mTOR-mediated activation of p70 S6K induces differentiation of pluripotent human  
45  
46 638 embryonic stem cells. *Cell Reprogram.* 2010; 12:263-73.  
47  
48  
49 639 38. Gangloff YG, Mueller M, Dann SG, Svoboda P, Sticker M, Spetz JF, et al. Disruption of  
50  
51 640 the mouse mTOR gene leads to early postimplantation lethality and prohibits embryonic  
52  
53 641 stem cell development. *Mol Cell Biol.* 2004; 24:9508-16.  
54  
55  
56  
57  
58  
59  
60  
61  
62  
63  
64  
65

- 642 39. Murakami M, Ichisaka T, Maeda M, Oshiro N, Hara K, Edenhofer F, et al. mTOR is  
1  
2 643 essential for growth and proliferation in early mouse embryos and embryonic stem cells.  
3  
4 644 Mol Cell Biol. 2004; 24:6710-18.  
5  
6  
7 645 40. Valli A, Rosner M, Fuchs C, Siegel N, Bishop CE, Dolznig H, et al. Embryoid body  
8  
9 646 formation of human amniotic fluid stem cells depends on mTOR. *Oncogene*. 2010;  
10  
11 647 18;29(7):966-77.  
12  
13  
14 648 41. Vosough M, Omidinia E, Kadivar M, Shokrgozar MA, Pournasr B, Aghdami N.  
15  
16 649 Generation of functional hepatocyte-like cells from human pluripotent stem cells in a  
17  
18 650 scalable suspension culture. *Stem Cells Dev*. 2013; 22:2693-705.  
19  
20  
21 651 42. Plageman TFJr, Chung MI, Lou M, Smith AN, JHildebrand JD, Wallingford JB, et al.  
22  
23 652 Pax6-dependent Shroom3 expression regulates apical constriction during lens placode  
24  
25 653 invagination. *Development*. 2010; 137:405-15.  
26  
27  
28 654 43. Hiscox S, Jiang WG. Ezrin regulates cell-cell and cell-matrix adhesion, a possible role  
29  
30 655 with Ecadherin/b-catenin. *J Cell Sci*. 1999; 112:3081-90.  
31  
32  
33 656 44. Deng B, Fang J, Zhang X, Qu L, Cao Z, Wang B. Role of gelsolin in cell proliferation  
34  
35 657 and invasion of human hepatocellular carcinoma cells. *Gene*. 2015; 571:292-97.  
36  
37  
38 658 45. Besse F, Mertel S, Kittel RJ, Wichmann C, Rasse TM, Sigrist SJ, et al. The Ig cell  
39  
40 659 adhesion molecule Basigin controls compartmentalization and vesicle release at  
41  
42 660 *Drosophila melanogaster* synapses. *J Cell Biol*. 2007; 177:843-55.  
43  
44  
45 661 46. Honda K, Yamada T, Endo R, Ino Y, Gotoh M, Tsuda H, et al. Actinin-4, a novel actin-  
46  
47 662 bundling protein associated with cell motility and cancer invasion. *J Cell Biol*. 1998;  
48  
49 663 140:1383-93.  
50  
51  
52 664 47. Lu J, Lian G, Lenkinski R, De Grand A, Vaid RR, Bryce T, et al. Filamin B mutations  
53  
54 665 cause chondrocyte defects in skeletal development. *Hum Mol Genet*. 2007; 16:1661-75.  
55  
56  
57  
58  
59  
60  
61  
62  
63  
64  
65

- 666 48. Tamura N, Ohno K, Katayama T, Kanayama N, Sato K. The PDZ-LIM protein CLP36 is  
1 required for actin stress fiber formation and focal adhesion assembly in BeWo cells.  
2 667  
3  
4 668 Biochem Biophys Res Commun. 2007; 364:589-94.  
5  
6  
7 669 49. Ryu JR, Echarri A, Li R, Pendergast AM. Regulation of cell-cell adhesion by  
8  
9  
10 670 Abi/Diaphanous complexes. Mol Cell Biol. 2009; 29:1735-48.  
11  
12 671 50. Sugiyama N, Gucciardo E, Tatti O, Varjosalo M, Hyytiäinen M, Gstaiger M, et al.  
13  
14 672 EphA2 cleavage by MT1-MMP triggers single cancer cell invasion via homotypic cell  
15  
16 673 repulsion. J Cell Biol. 2013; 201:467-84.  
17  
18  
19 674 51. Balasubramanian N, Meier JA, Scott DW, Norambuena A, White MA, Schwartz MA.  
20  
21 675 RalA-exocyst complex regulates integrin-dependent membrane raft exocytosis and  
22  
23 676 growth signaling. Curr Biol. 2010; 20: 75-79.  
24  
25  
26 677 52. Allaire PD, Seyed SM, Chaineau M, Seyed SE, Konefal S, Fotouhi M, et al. Interplay  
27  
28 678 between Rab35 and Arf6 controls cargo recycling to coordinate cell adhesion and  
29  
30 679 migration. J Cell Sci. 2003; 126:722-31.  
31  
32  
33  
34 680  
35  
36

## 681 **Figure legends**

682 **Figure 1.** Autophagy machinery is widely operated in iPSCs. (A) Images of cells were taken at  
683 day 15 of fibroblast reprogramming and large autophagic vacuoles were arrowheaded. (B)  
684 Smaller autophagic vacuoles (arrowheaded) were observed in stable iPSC lines with daily  
685 change of culture medium. (C-D,G-H) Double immunofluorescence staining of iPSCs (C-D) and  
686 fibroblasts (G-H) was carried out with anti-LC3B for autophagy (C,G, green) and anti-LAMP1  
687 for lysosome (C,G, red), Syntaxin 6 for Golgi membrane (D,H, red) and MitoGreen (D, H,  
688 green) for mitochondria, with counter-staining of DAPI (blue) for nuclei. Fluorescent images  
689 were acquired *via* confocal microscopy. Note that LC3B and LAMP1 are colocalized in iPSCs  
690 (C) but not in fibroblasts (G), whereas Syntaxin 6/MitoGreen are not colocalized as anticipated

691 (D,H). (E, I-L) Transmission electronic microscopic images showed a dead nucleus (\*, A and  
692 E), lysosomal structures (blue arrowheads, E,I), and autophagic vacuoles (red arrowheads, J-L).  
693 Bars=20  $\mu$ m in A-D and F-H; 10  $\mu$ m in E and I; 500 nm in J-L.

694 .  
695 **Figure 2.** iPSCs exhibit higher autophagy activity than parental fibroblasts. Fibroblasts (a-d, a'-  
696 d') and iPSCs (A-D, A'-D') derived from 4 independent donors were culture in the absence (-R)  
697 or presence (+R) of 100nM Rapamycin for 24 hours. The iPSCs showed higher basal staining of  
698 LC3B (A-D) than in parental fibroblasts (a-d). LC3B was highly induced by 100 nM of  
699 Rapamycin in iPSCs (A'-D'), with lower levels of induction in their respective fibroblasts (a'-  
700 d'). Fluorescent images were acquired *via* confocal microscopy. Bar=10  $\mu$ m. (E) Immunoblots of  
701 the protein extracts from untreated (-R) or treated (+R) cells with anti-LC3B-II and anti- $\beta$ -  
702 ACTIN. (F-G) The relative abundance of LC3B-II was quantified using ImageJ and data were  
703 presented with Mean  $\pm$  SD. (F) The basal level of LC3B-II in the iPSCs was 2.55-fold higher  
704 than in parental fibroblasts (\*\*,  $p < 0.01$ , n=4). (G) Rapamycin-induced expression of LC3B-II in  
705 the iPSCs was also 2.23-fold higher than fibroblasts (\*,  $p < 0.05$ , n=4).

706  
707 **Figure 3.** Wide expression of different autophagy components in independent iPSC lines.  
708 Proteins were extracted from iPSCs with daily renewal of culture medium. 15  $\mu$ g of protein was  
709 loaded onto each lane. Lane a-l represents 12 independent iPSC lines from 10 donors (a, 33D6;  
710 b, JOM; c, LV1; d, LV2; e, LV3; f, 001CC1; g, NRXN1C1; h, 002V; I, 003V; j, SC126; k,  
711 SC128, l, SC132). (A-C) Immunoblotting was carried out with antibodies against LC3B-I,  
712 LC3B-II, BECLIN-1, AMPK $\alpha$ , ULK1, ULK2, ATG3, ATG12, ATG13, ATG101 and  $\beta$ -Actin.  
713 (D-G) The relative abundance of the proteins was quantified using ImageJ against  $\beta$ -Actin and  
714 data were presented with Mean  $\pm$  SD. (H) Immunoblots were carried out to compare expression

715 of ATG5 and ATG 12 among 3 fibroblast lines (3x Fib.) and 5 iPSC lines (5xiPSCs) of healthy  
716 donors, showing higher ATG5 and ATG12 expression in iPSCs than that in fibroblasts.

717  
718 **Figure 4.** Rapamycin induces autophagy in time- and concentration-dependent manners in  
719 iPSCs. iPSCs were maintained in 6-well plates and medium was renewed daily. Image of LC3B  
720 staining in panels A-D were taken from 4 days of Rapamycin treatment at 0, 10, 100 or 200 nM  
721 respectively, and image in panels E-H were sampled from 200 nM of Rapamycin treatment for 1,  
722 3 and 6 days respectively, showing concentration- and time-dependent induction. (I) Proteins  
723 were extracted from iPSCs treated with Rapamycin at 0, 1, 10, 100, 200 or 300 nM for 4 days,  
724 and immunoblotted with antibodies against LC3B, phosphorylated ULK1, phosphorylated p70  
725 S6K or  $\beta$ -Actin. (J-L) The relative abundance of the LC3B-II/I ratios (J), p-p70S6K (K) and p-  
726 ULK1 (L) was quantified using ImageJ against a loading control  $\beta$ -Actin. Data were presented  
727 with Mean  $\pm$  SEM, with \* for  $p < 0.05$ , and \*\* for  $p < 0.01$ . Bars = 10 $\mu$ m in A-H.

728  
729 **Figure 5. Rapamycin attenuates Bafilomycin A1-induced iPSC death.** iPSCs were treated with  
730 0 (A), 5nM (B) , 50 nM (C) , 100 nM (D,E) of Bafilomycin for 24 (A-D) or 48 hours (E).  
731 Bafilomycin A1 induced cell death in a concentration dependent manner (A-D), leading to  
732 substantial cell loss after 48 hours at 100 nM (D). Addition of 200 nM Rapamycin attenuate  
733 Bafilomycin A1-induced cell death and maintained iPSC normal cell density (F,G). (H) Anti-  
734 ACTIN and Anti-LC3B immunoblotting were carried out with iPSC lysates from control iPSCs  
735 (Con), or 24 hour of treatment with 200 nm of Rapamycin (Rap), or with 100 nM of Bafilomycin  
736 A1 (Baf) or with both (Rap+Baf). (I) The relative abundance of the LC3B-II/I ratios was  
737 quantified against a loading control  $\beta$ -ACTIN. Data were presented with Mean  $\pm$  SEM, with \*  
738 for  $p < 0.05$ , and \*\* for  $p < 0.01$ , n = 4. Bar=50  $\mu$ m in A-B.

740 **Figure 6.** A time course of Rapamycin-induced cell detachment and EB formation. iPSCs were  
1  
2 741 cultured in the presence of 200 nM Rapamycin. Bright field microscopic images were taken after  
3  
4 742 1 (B), 2 (C), 3 (D) and 6 (E-F) days of treatment. EB-like spheres were spontaneously formed  
5  
6  
7 743 after 6 days of Rapamycin treatment. Arrowheads in C, E and F indicated the border of the iPSC  
8  
9  
10 744 colonies which formed a line after day 6 to limit colony expansion sideways. (E) \* indicated the  
11  
12 745 areas of iPSC detachment, which were filled with a thin layer of iPSCs. (F) Four EB-like spheres  
13  
14 746 of comparable size were captured in the fields. (G) Magnified view (4x) of the border area  
15  
16  
17 747 arrowheaded in image F. Bar=100  $\mu\text{m}$  in A-D, 200  $\mu\text{m}$  in E-F.

18  
19  
20 748  
21  
22  
23 749 **Figure 7.** Rapamycin induces spontaneous formation of uniform sizes of EBs. (A-C) Images of  
24  
25 750 floating spheres appeared after 9 days of Rapamycin treatment (200 nM) from 3 iPSC lines. (D-  
26  
27  
28 751 F) Images of EBs made after 9 days from “cut-and-paste” method. (G) The EB area sizes ( $\mu\text{m}^2$ )  
29  
30 752 were quantified with ImageJ and data were presented with Mean  $\pm$  SD. Note the round shape and  
31  
32  
33 753 uniform sizes of EBs from Rapamycin treatment (A-C), in contrast to irregular shape and sizes  
34  
35 754 of EBs resulted from the same iPSC lines by mechanical method (D-F). Bar = 200  $\mu\text{m}$ .

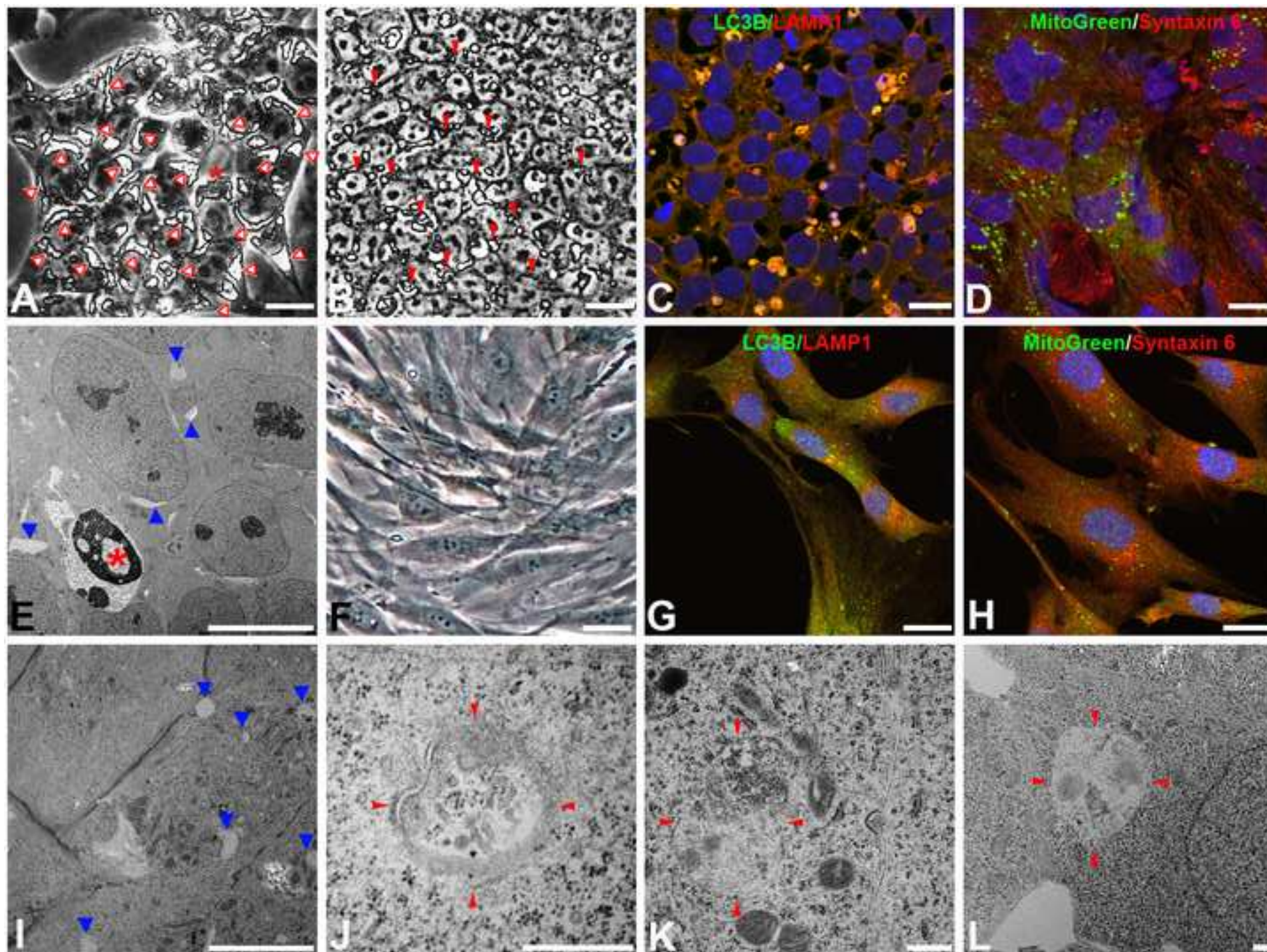
36  
37  
38 755  
39  
40  
41 756 **Figure 8.** Rapamycin treatment accelerates differentiation of human iPSCs in association with  
42  
43  
44 757 decreased NANOG expression. (A) Proteins were extracted from Rapamycin-induced spheres  
45  
46 758 and control EBs, and blotted with antibodies against LC3B, AFP, ASM, TUJ1 and  $\beta$ -ACTIN. (B)  
47  
48  
49 759 Relative protein expression was quantified against  $\beta$ -ACTIN, (C) compared between two  
50  
51 760 methods, and presented as M  $\pm$  SEM. Note a 2~3 fold increase of LC3B, AFP, ASM, and TUJ1  
52  
53  
54 761 expression in Rapamycin-induced spheres. Rapamycin-induced spheres and control EBs were  
55  
56 762 plated out for spontaneous differentiation for 3 days (J-K) or 5 day (D-I), and stained for  
57  
58  
59 763 NESTIN (M), TUJ1 (D, G), ASM (E, H), AFP (E, I). Note the presence of more immune-



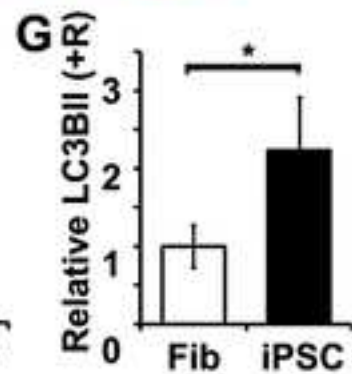
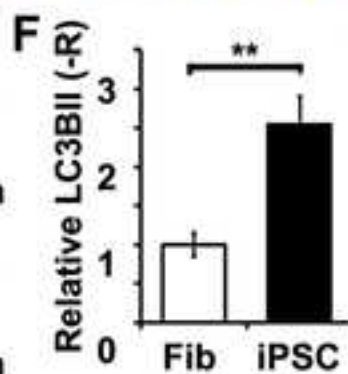
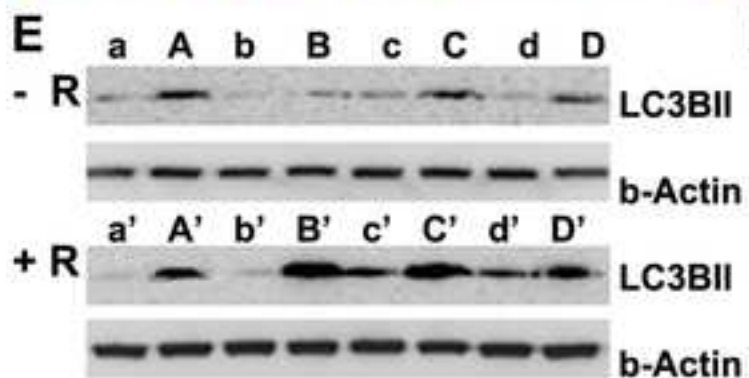
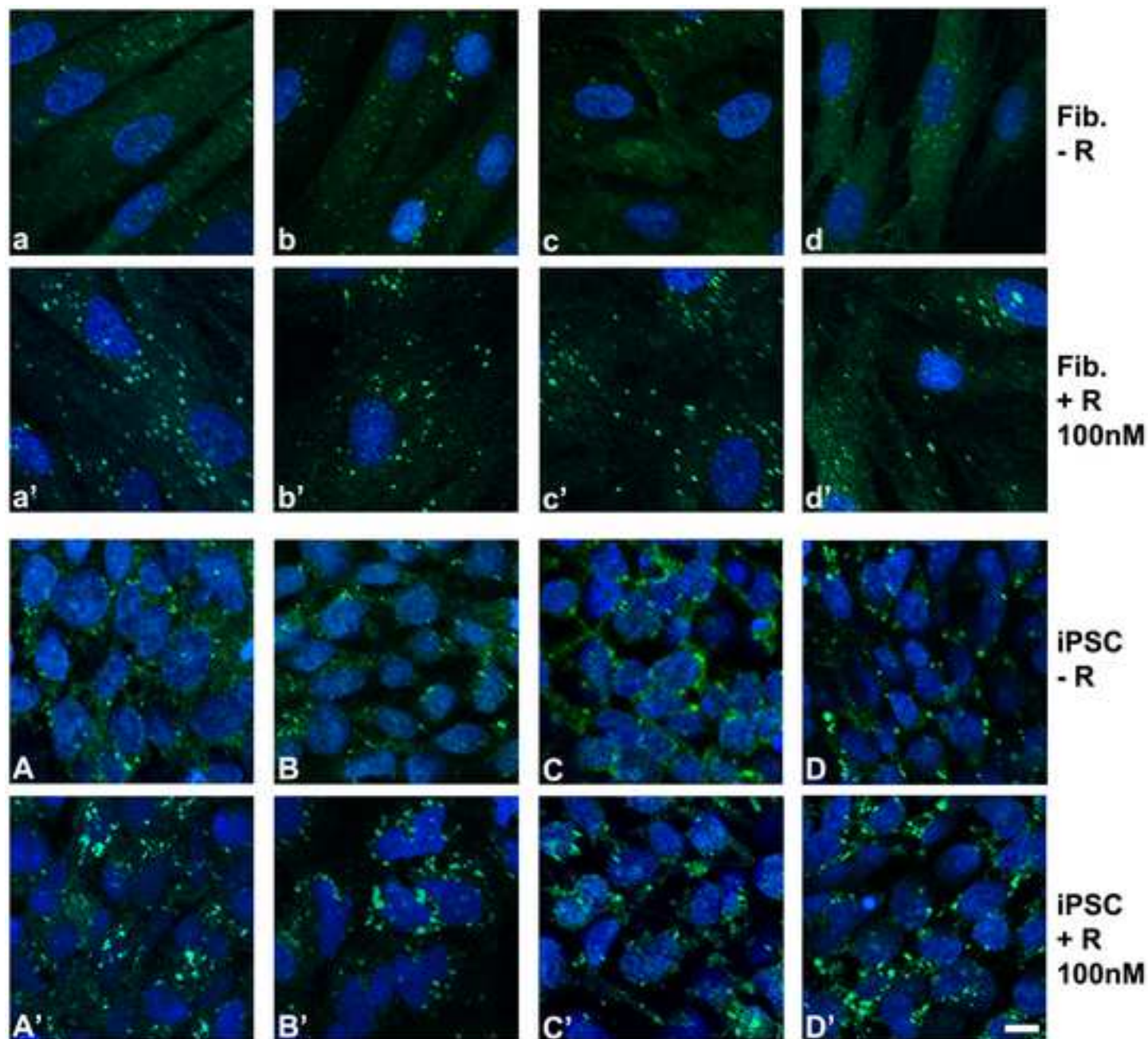
764 positive cells in derivatives of Rapamycin-induced spheres (G-I) compared with cells  
765 differentiated from conventional EBs (E-F). (L) Proteins were extracted from iPSCs treated with  
766 Rapamycin at 0, 1, 10, 100, 200 or 300 nM for 4 days, and immunoblotted with anti-NANOG,  
767 showing concentration-dependent reduction of NANOG expression after Rapamycin treatment.  
768 (M) Relative abundance of NANOG expression after 4 days of Rapamycin treatment. Bar = 100  
769  $\mu\text{m}$  in D-I; Bar = 50  $\mu\text{m}$  in J-K. \* for  $p < 0.05$ , and \*\* for  $p < 0.01$ .

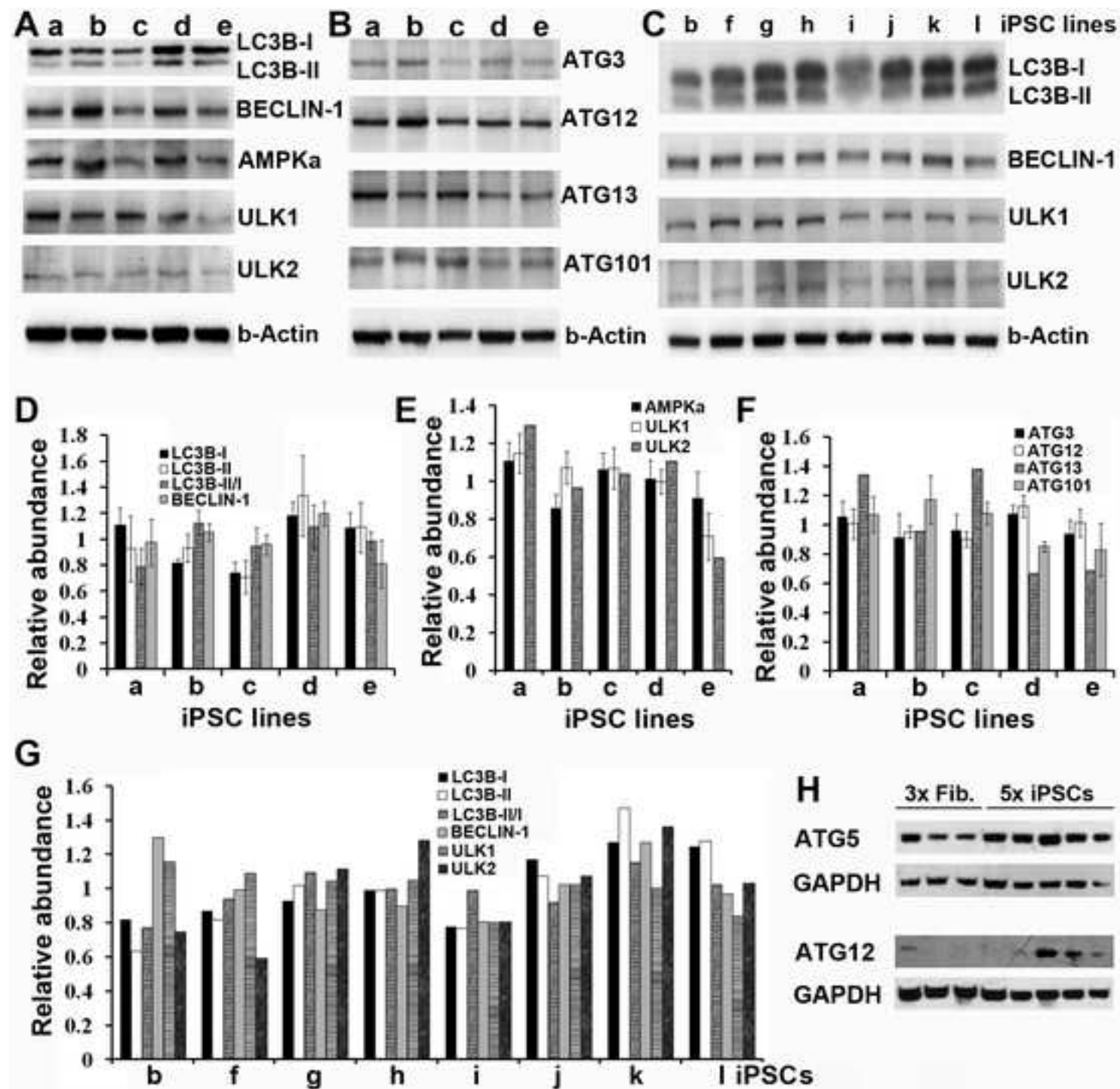
771 **Figure 9.** Rapamycin regulates adherens junctions and actin cytoskeleton pathways in iPSCs.  
772 Three independent lines of iPSCs were maintained in mTeSR™ (con) or in the presence of 50 or  
773 100nm Rapamycin for 3, 6 or 9 days. Proteins were harvested for Mass Spectrometry analyses.  
774 (A-E) The time course changes of protein expression (mean $\pm$ SEM, n=3). \* for  $p < 0.05$ . (F) The  
775 molecular network for selected proteins whose expression was altered. The data show the  
776 network of interactions between adherens junctions and actin signaling by the STRING. The  
777 arrows indicated up- or down-regulation of the protein expression after Rapamycin treatment.

779 **Supplemental Figure 1. Rapamycin induces LC3B expression in human fibroblasts.** Three  
780 lines of human fibroblasts (F1, F2, F3) were treated without (-) or with (+) 100 nM Rapamycin  
781 overnight. The protein lysates were run of 15% SDS-PAGE and blotted with anti-LC3B and anti-  
782 GAPDH. Two bands of LC3B-I (16kD) and LC3B-II (14kD) were seen. Rapamycin is shown to  
783 induce LC3B-I expression after 24 hours of treatment.

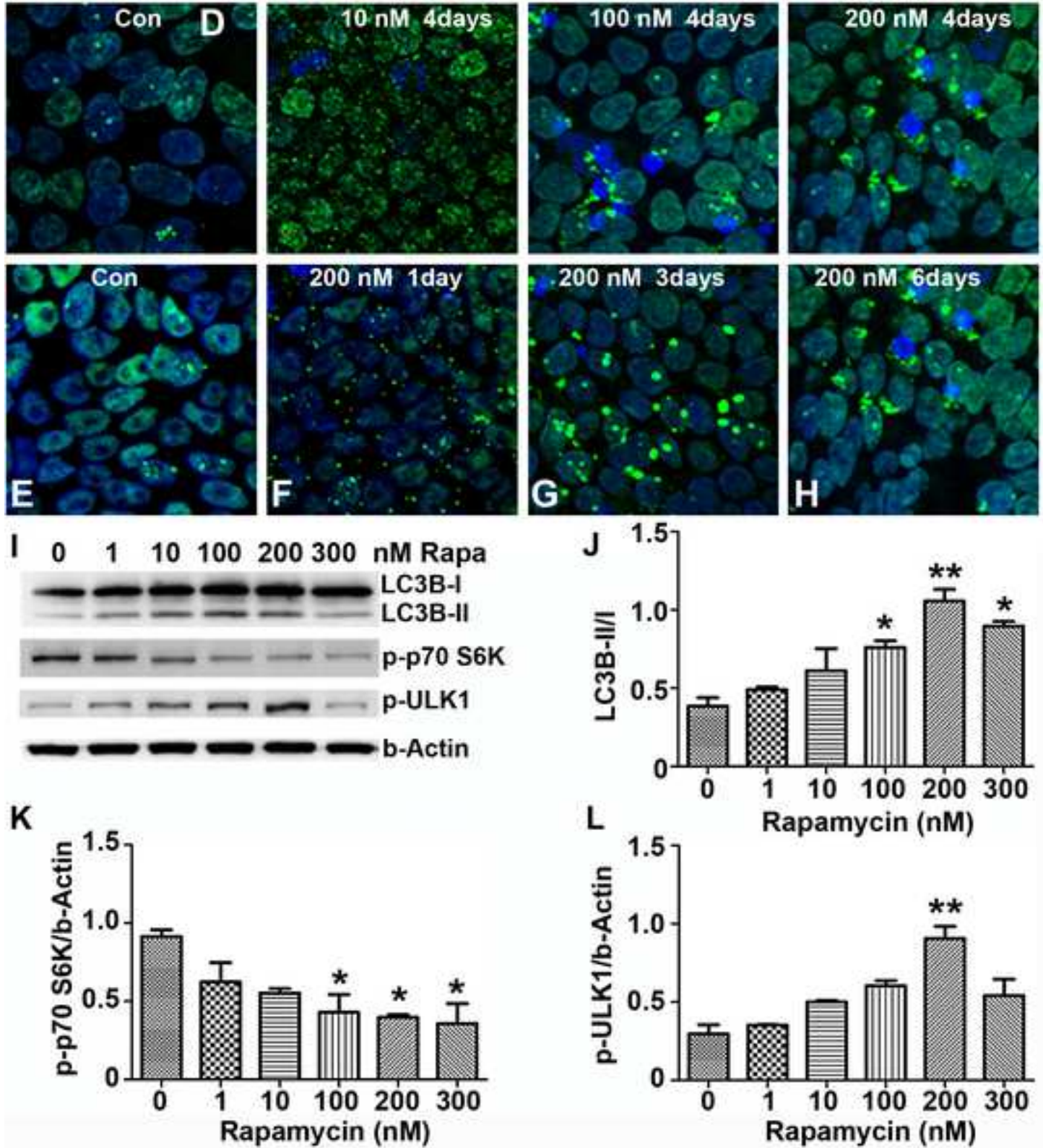




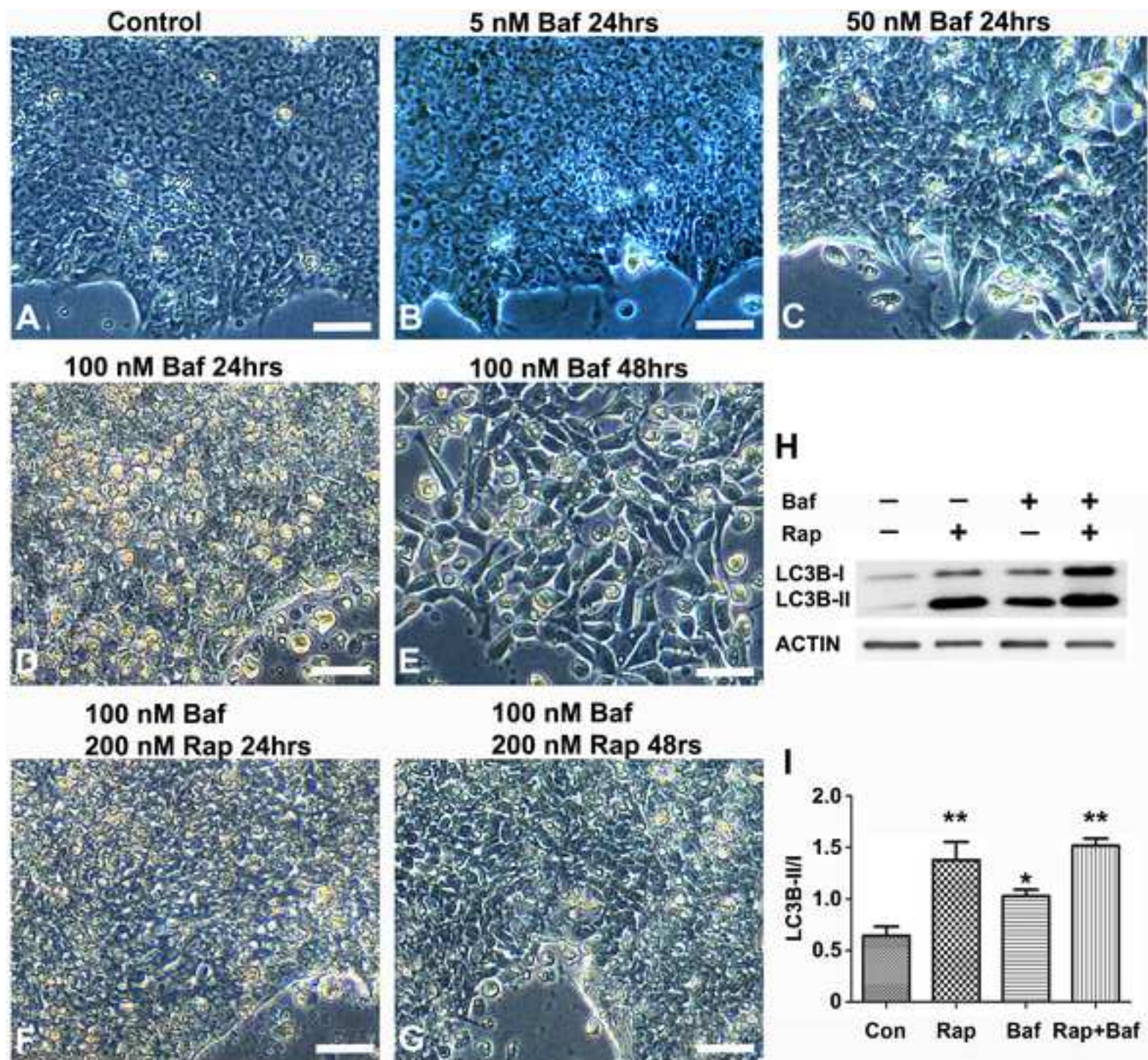




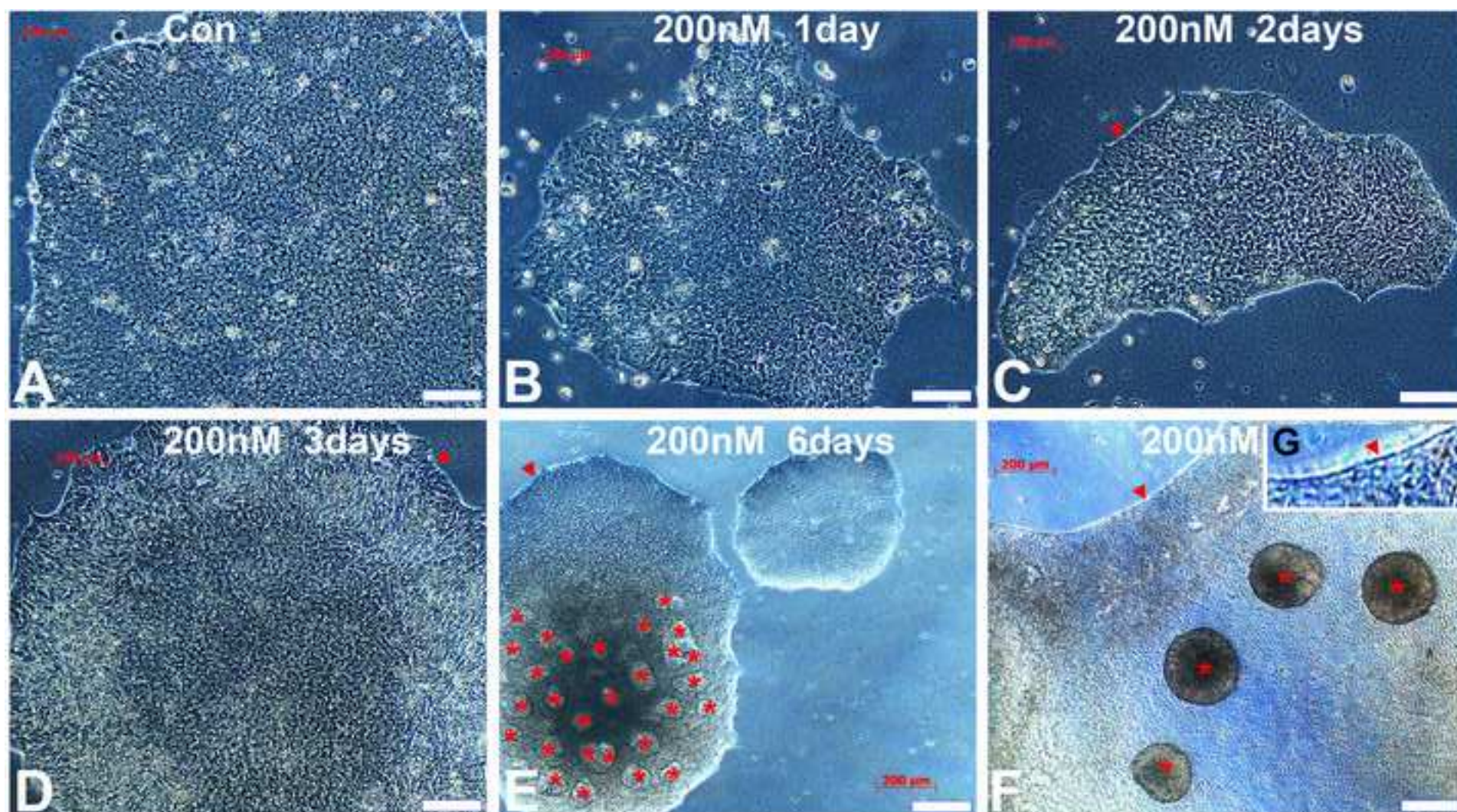




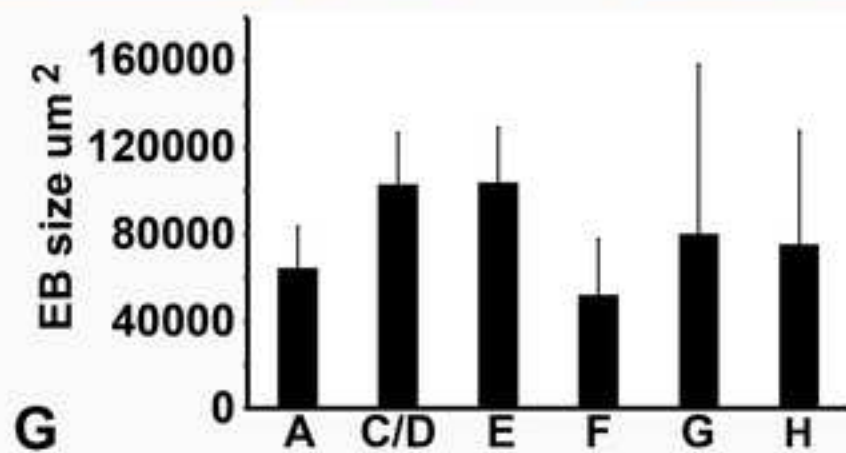
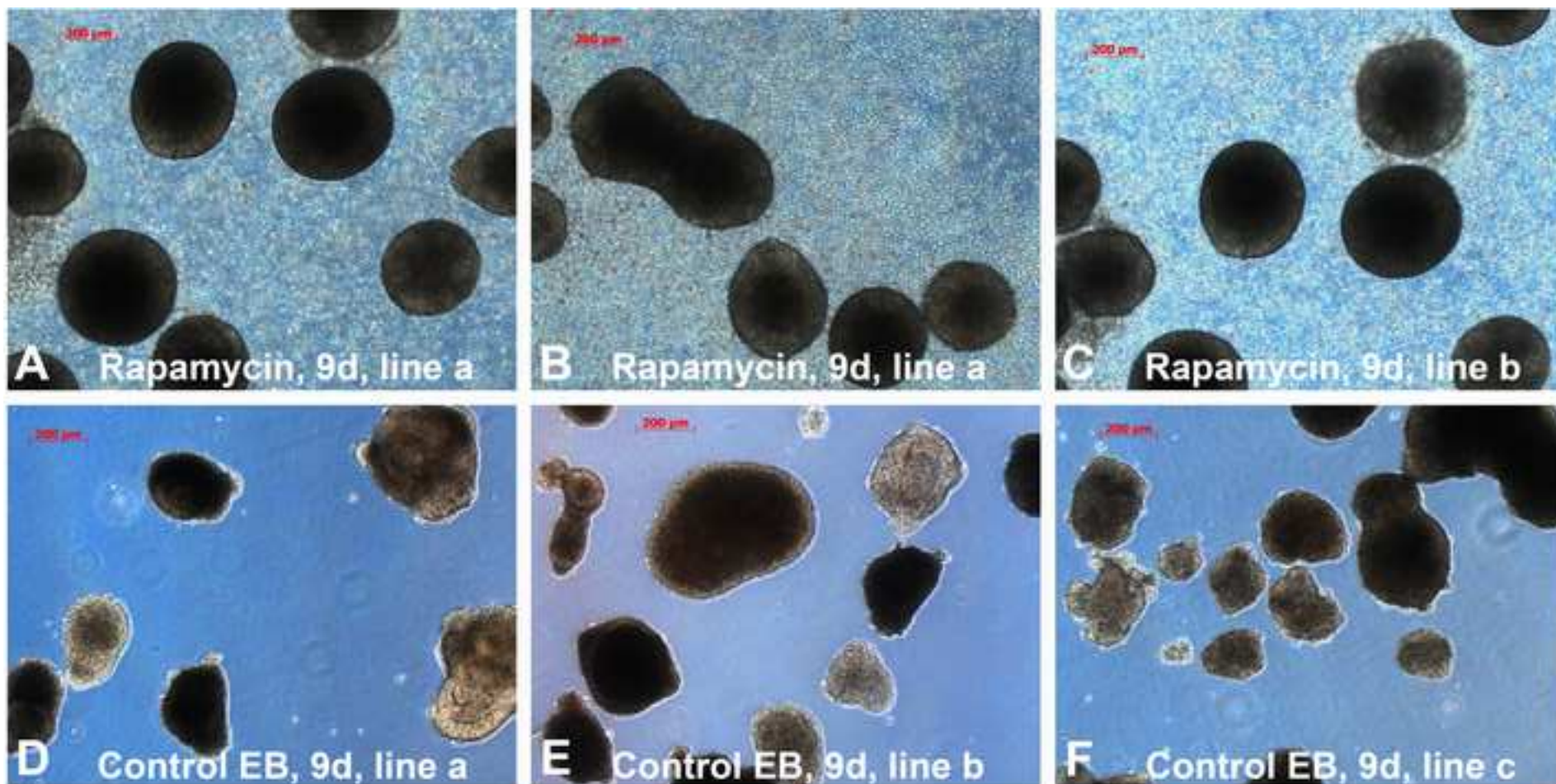




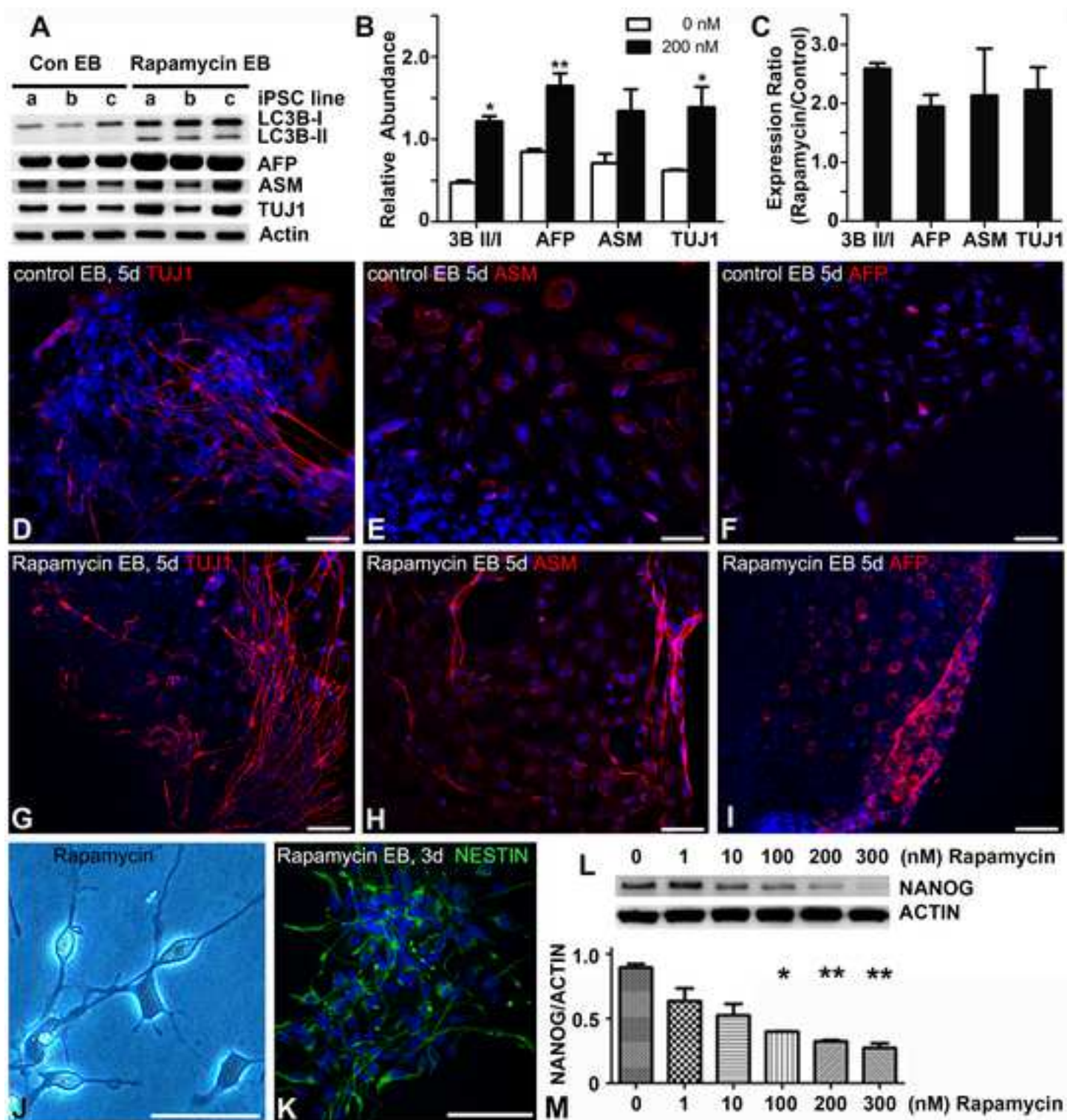


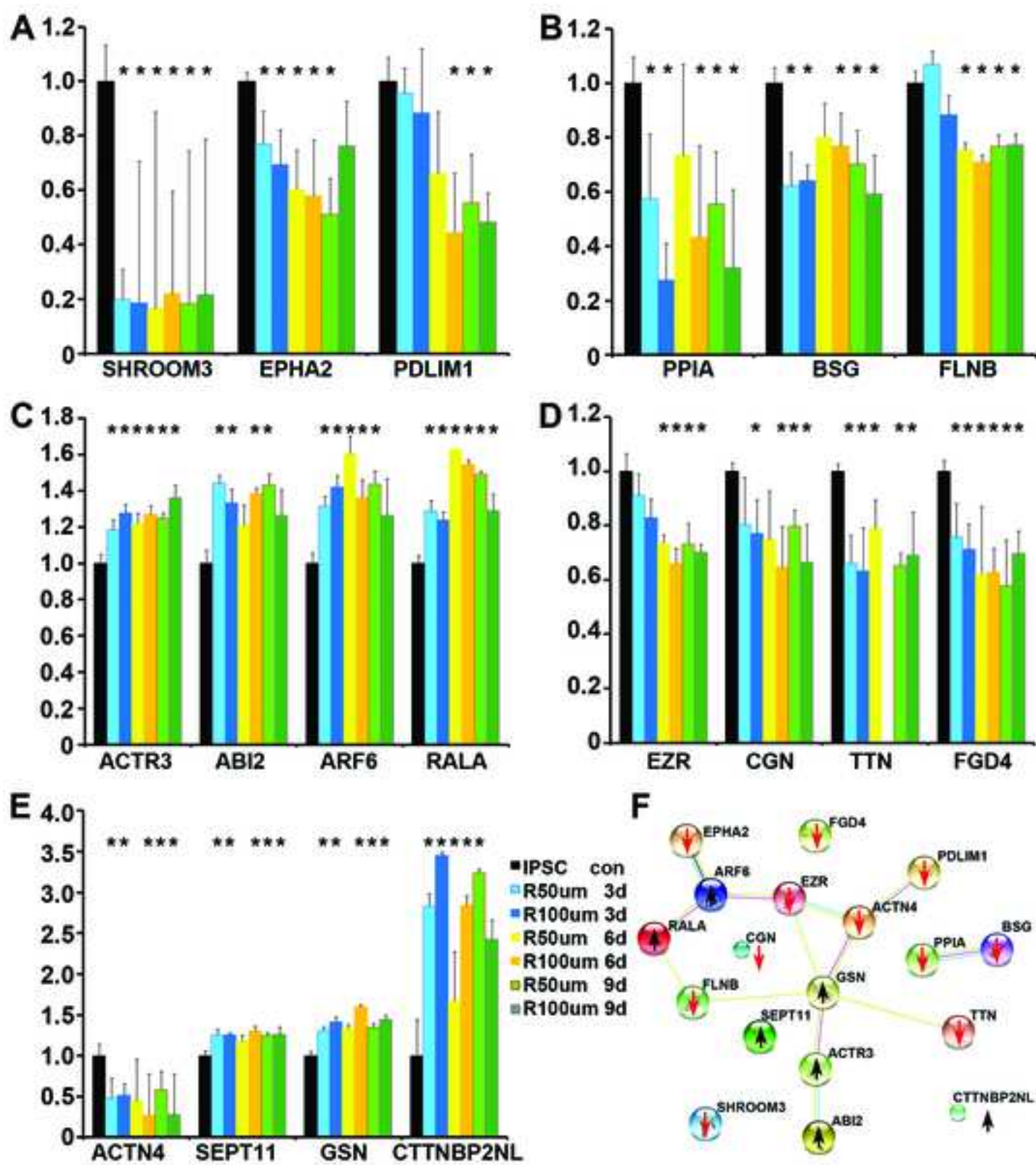














Click here to access/download  
**Supplementary Material**  
Suppl Fig 1 Fibroblasts+Rapmycin.tif





Submission of Revised Manuscript: **“Rapamycin Regulates Autophagy and Cell Adhesion in Induced Pluripotent Stem Cells”**

Dear Editor,

We thank you very much for your kind invitation. We have done additional experiments to carry out a comprehensive revision for the manuscript **“Rapamycin Regulates Autophagy and Cell Adhesion in Induced Pluripotent Stem Cells”** by Sothibundhu *et al*, with point-to-point response to address

Reviewers’ constructive comments. The texts are revised accordingly with key revision data including:

Figure 1: we have provided fibroblasts image in Figure 1F and double staining images in Figure 1C.D.G.H.

Figure 3: we have supplied comparison with fibroblasts in Figure 3H by immunoblotting.

Figure 5: we added new Bafilomycin treatment data Figure 5A-I.

Figure 7: we removed duplicated image in Figure 7.

Figure 8: we removed duplicated images and supplied new mechanistic data of NANOG expression in Figure 8L-M.

Supplemental Figure 1: Immunoblotting of fibroblasts for LC3B expression.

We hope the revised manuscript has addressed major concerns and comments in the previous review process.

We will be delighted to hear if the manuscript has now reached the standard of SCRT for publication.

Kind regards

A handwritten signature in black ink, appearing to read "Sanbing Shen".

Sanbing Shen, PhD  
Professor of Fundamental Stem Cell Biology,  
Regenerative Medicine Institute,  
School of Medicine, National  
University of Ireland Galway (NUI) Ireland.  
Tel: 00-353-91-494261 (office).  
Email: [sanbing.shen@nuigalway.ie](mailto:sanbing.shen@nuigalway.ie).